THE JOURNAL OF BIOLOGICAL CHEMISTRY VOL. 291, NO. 32, pp. 16686–16698, August 5, 2016

Synthetic Lethal Screen Demonstrates That a JAK2 Inhibitor Suppresses a BCL6-dependent IL10RA/JAK2/STAT3 Pathway in High Grade B-cell Lymphoma*

Received for publication, May 6, 2016, and in revised form, June 5, 2016 Published, JBC Papers in Press, June 6, 2016, DOI 10.1074/jbc.M116.736868

Daniel Beck[‡1], Jenny Zobel[§1,2], Ruth Barber[‡¶1], Sian Evans[‡3], Larissa Lezina[‡], Rebecca L. Allchin[‡4], Matthew Blades[‖], Richard Elliott[**], Christopher J. Lord[**], Alan Ashworth[**], Andrew C. G. Porter[§2], and Simon D. Wagner[‡2,5]

From the [‡]Department of Cancer Studies, Ernest and Helen Scott Haematology Research Institute, and [¶]Leicester Diagnostic and Drug Development (LD3) Centre, University of Leicester, Lancaster Road, Leicester LE1 7HB, [§]Department of Haematology, Imperial College London, Hammersmith Campus, Du Cane Road, London W12 0NN, [‖]Bioinformatics and Biostatistics Analysis Support Hub (B/BASH), University of Leicester, Lancaster Road, Leicester LE1 9HN, and [**]The Breakthrough Breast Cancer Research Centre, The Institute of Cancer Research, 237 Fulham Road, London SW3 6JB, United Kingdom

We demonstrate the usefulness of synthetic lethal screening of a conditionally BCL6-deficient Burkitt lymphoma cell line, DG75-AB7, with a library of small molecules to determine survival pathways suppressed by BCL6 and suggest mechanism-based treatments for lymphoma. Lestaurtinib, a JAK2 inhibitor and one of the hits from the screen, repressed survival of BCL6-deficient cells *in vitro* and reduced growth and proliferation of xenografts *in vivo*. BCL6 deficiency in DG75-AB7 induced JAK2 mRNA and protein expression and STAT3 phosphorylation. Surface IL10RA was elevated by BCL6 deficiency, and blockade of IL10RA repressed STAT3 phosphorylation. Therefore, we define an IL10RA/JAK2/STAT3 pathway each component of which is repressed by BCL6. We also show for the first time that JAK2 is a direct BCL6 target gene; BCL6 bound to the JAK2 promoter *in vitro* and was enriched by ChIP-seq. The place of JAK2 inhibitors in the treatment of diffuse large B-cell lymphoma has not been defined; we suggest that JAK2 inhibitors might be most effective in poor prognosis ABC-DLBCL, which shows higher levels of IL10RA, JAK2, and STAT3 but lower levels of BCL6 than GC-DLBCL and might be usefully combined with novel approaches such as inhibition of IL10RA.

There is a need for new treatments for poor-prognosis activated B-cell-like diffuse large B-cell lymphoma (ABC-DLBCL),[6] which continues to have a cure rate <40% with conventional chemotherapy (1).

The majority of ABC-DLBCL, in contrast to germinal center B-cell-like DLBCL, have low level expression of BCL6 mRNA and protein (2). JAK/STAT3 signaling is active in ABC-DLBCL and is enhanced by constitutive activity of the NF-κB pathway (3), which in turn is driven by oncogenic CARD11 mutations (4), chronic active B-cell receptor signaling (5), and MYD88 mutations (6). However, other factors are also likely to be important in determining the overall activity of JAK/STAT3 signaling. BCL6 directly represses both STAT3 (7) and NF-κB p105/p50 (8) transcription, and levels of BCL6 might, therefore, be a factor independent of the known oncogenic mutations, which determines the activity of signaling pathways required by ABC-DLBCL. In this report we develop a novel B-cell line to pursue the hypothesis that genes repressed by BCL6 are components of survival signaling pathways in lymphomas with low level expression of this transcription factor.

BCL6 is a zinc finger transcription factor that is highly expressed in normal germinal center B-cells (9) and is required for high affinity antibody production (10, 11). It is also constitutively expressed in ~40% of cases of the high grade B-cell lymphoma DLBCL due to either chromosomal translocations, mutations of a negative regulatory site in the promoter region (12–14), or abnormalities of post-translational regulation (15–17).

The N-terminal POZ domain of BCL6 associates with co-repressors NCOR1, BCOR, and SMRT (NCOR2), which in turn recruit histone deacetylases to accomplish transcriptional repression. Work largely carried out with human Burkitt lymphoma cell lines and mouse B-cell lines showed that BCL6 represses B-cell terminal differentiation through a direct effect on BLIMP1 (PRDM1) (18–20). Effects on the cell cycle have been less clearly defined; BCL6 represses cyclin D2 transcription (18), but it also suppresses the cyclin-dependent kinase inhibitor p21 (21) and in primary cells prevents senescence and induces cyclin D1 (22). Suppression of DNA damage responses and p53 by BCL6 are believed to be required to allow somatic hypermutation in normal germinal center B-cells (23, 24). As mentioned above, STAT3 and NF-κB, which are both required by ABC-DLBCL, are direct targets of BCL6 transcriptional repression (7, 8).

* This work was supported by a grant from Leukemia and Lymphoma Research (to S. D. W.). The authors declare that they have no conflicts of interest with the contents of this article.

Microarray data have been submitted to GEO with accession number GSE55301.

[1] These authors contributed equally to this work.

[2] A Gordon Piller Leukaemia and Lymphoma Research PhD Studentship to S. D. W. and A. C. G. P. supported J. Z.

[3] Supported by a University of Leicester Ph.D. Studentship.

[4] Supported by a Clinical Research Fellowship from the Ernest and Helen Scott Hematology Research Institute.

[5] To whom correspondence should be addressed: Dept. of Cancer Studies, Rm. 104, Hodgkin Bldg., University of Leicester, Lancaster Rd., Leicester LE1 7HB, UK. Tel.: 441162525584; Fax: 441162525616; E-mail: sw227@le.ac.uk.

[6] The abbreviations used are: ABC-DLBCL, activated B-cell-like diffuse large B-cell lymphoma(s); Gy, gray; ATR, ATM and Rad3-related; GC, germinal center.

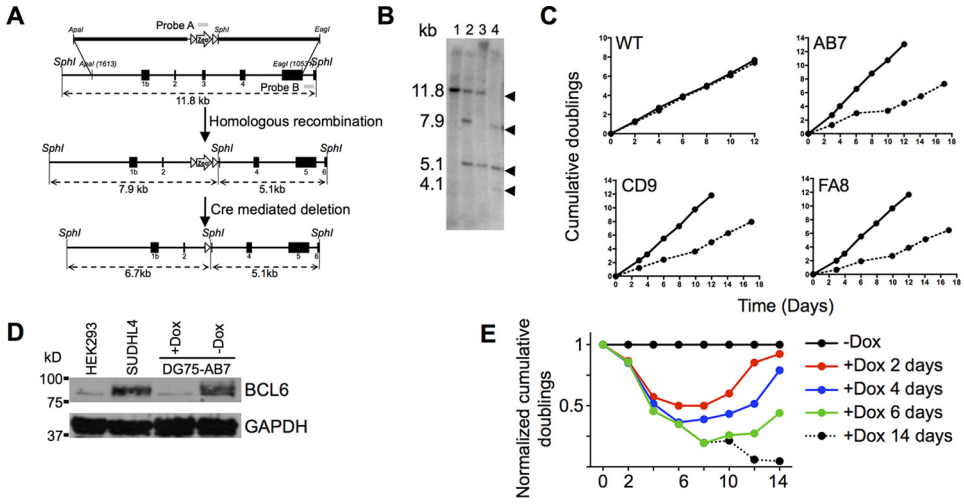

FIGURE 1. **A conditional BCL6-deficient human B-cell line.** *A*, scheme of disruption of the endogenous BCL6 loci of DG75. A zeocin resistance cassette flanked by *lox*P sites was inserted into exon 3 of the BCL6 gene, containing the initiation codon by homologous recombination. After Cre recombinase mediated removal of the antibiotic resistance gene the process was repeated on the second BCL6 allele. *B*, Southern demonstrating disruption of the endogenous BCL6 loci and the presence of the inserted BCL6 transgene. Genomic DNA was digested with SphI and probed with labeled probes A and B. Wild-type cells ($BCL6^{+/+}$, *lane 1*) gave an 11.8-kb band. After the first round of targeting and before removal of the zeocin resistance cassette ($BCL6+/-$ Zeo^r, *lane 2*) the 11.8 kb band was present with 7.9-kb and 5.1-kb bands from the targeted locus. After removal of the zeocin resistance cassette but before targeting of the second locus ($BCL6^{+/-}$, *lane 3*) 11.8-kb and 5.1-kb bands were present. After insertion of the BCL6 transgene and targeting of the second locus ($BCL6^{-/-}$ Zeo^r + pTRE-BCL6HA, *lane 4*) the 11.8-kb band was no longer present, bands of 7.9 kb and 5.1 kb from the disrupted BCL6 loci were present together with a band of 4.1 kb from the BCL6 transgene. *C*, growth curves (cumulative doublings) of wild-type DG75 (WT) and three targeted clones (AB7, CD9, and FA8) in the absence (*solid line*) and presence (*dotted line*) of doxycycline. *D*, Western showing BCL6 expression in DG75-AB7 in the presence and absence of doxycycline. BCL6 expression in the DLBCL cell line, SUDHL4 (BCL6 expressing), and HEK293 cells (BCL6 non-expressing) are also shown. *E*, the effects of doxycycline on proliferation are reversible. DG75-AB7 cells were cultured in the presence or absence of doxycycline or with doxycycline for various times (2, 4, or 6 days) before exchanging with culture medium lacking the antibiotic. Proliferation rate (cumulative doublings) were normalized to proliferation of cells cultured without doxycycline.

We engineered a conditional BCL6-deficient human B-cell line, DG75-AB7, from an EBV-negative Burkitt lymphoma cell line proficient for homologous recombination, DG75 (25, 26). We employed DG75-AB7 in a synthetic lethal screen to determine compounds inhibiting pathways that are active in BCL6-deficient cells. Synthetic lethal screening has previously been employed to find agents that are preferentially effective in the killing of cell lines bearing a transforming mutation (27) and is more widely the basis for siRNA and high throughput drug screens to discover novel therapeutics for cancer (28).

For this study we defined synthetic lethality as reduction of survival of BCL6-deficient DG75-AB7 cells while relatively sparing BCL6-replete cells. To carry out the synthetic lethal screen we employed a library of small molecule inhibitors that are either in clinical use or are good candidates for clinical use. Hits from the screen could, therefore, potentially be rapidly introduced into clinical trials. We demonstrate that IL10RA and JAK2 are transcriptionally regulated by BCL6 and suggest (7, 29) that low BCL6 is a determinant of an IL10RA/JAK2/STAT3 pathway that might be important in survival of some ABC-DLBCL.

Results

Characterization of a Conditional BCL6-deficient B-cell Line—BCL6 deficiency reduces survival and causes accumulation in G_1.

We produced conditional BCL6-deficient Burkitt lymphoma cell lines. On the addition of doxycycline BCL6 was effectively repressed, and proliferation was reduced in three separate clones (Fig. 1, *C* and *D*). Further work was carried out with clone DG75-AB7. When doxycycline was washed out of the culture medium, the effects on growth were reversed, suggesting a continuing requirement for BCL6 (Fig. 1*E*). After 7 days of culture doxycycline-treated DG75-AB7 cells had undergone fewer cell divisions than untreated cells (Fig. 2*A*) with an accompanying reduction in survival and an increase in cells in G_1 at the expense of G_2M and S phases (Fig. 2*B*). Overall BCL6-deficient cells showed reduced proliferation due to G_1 growth arrest.

Gene expression profiling was carried out to obtain a comprehensive view of BCL6 gene target alterations in DG75-AB7. 205 genes with a ≥2-fold up- or down-regulation in at least one of the samples cultured with doxycycline (16, 48, or 96 h) compared with the basal (−doxycycline) sample were identified. 14/205 genes were not annotated and were hence excluded from subsequent analysis, leaving 191 genes. Of these, 162 genes (85%) were up-regulated in response to BCL6 depletion (Table 1). Validation by RT-polymerase chain reaction (PCR) was carried out for a subset of these genes (Fig. 3 and Table 2).

To identify biological pathways altered in response to BCL6 depletion, functional annotation clustering was carried out (32, 33). Cell cycle gene CDKN1B (p27kip2), a previously identified BCL6 target gene 18, was up-regulated together with other regulators of cell cycle progression (CDC25A, CDC6, E2F8, and RB1). Other pathways regulated by BCL6 were B-cell receptor signaling (SYK, BLNK, PTPRC (CD45), IFITM1 (LEU13 or CD225), CD72 and PTPN6 (SHP1)) and calcium signaling (CYSLTR1 (GPCR), ATP2A (SERCA1), ITPR1/ITPR2 (IP3R), CAMK4 and PTK2B (FAK2, Pyk2)).

Work by others has demonstrated specific functionally important BCL6 targets (18). Analysis of changes in DG75-AB7

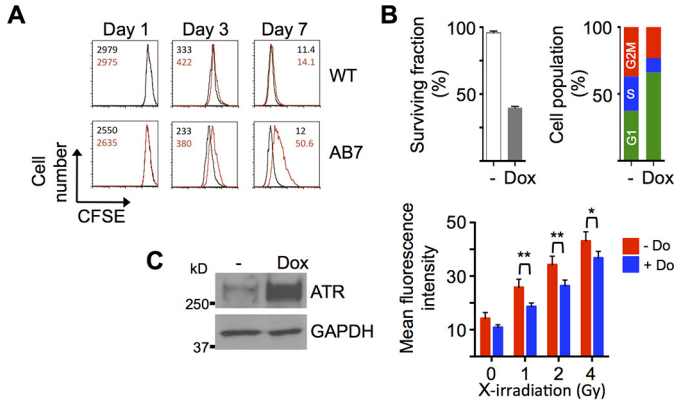

FIGURE 2. **Characterization of DG75-AB7.** *A*, BCL6 deficiency caused a defect in proliferation. Wild-type DG75 (*WT*) and DG75-AB7 (*AB7*) were loaded with carboxy fluorescein succinimidyl ester (*CSFE*), and fluorescence was measured in the absence (*black line*) or presence (*red line*) of doxycycline over the course of 7 days. Fluorescence histograms are presented. Mean fluorescence intensity is indicated in the *top left corner*. *B*, surviving fraction of DG75-AB7 after culture with doxycycline measured by a luminescence cell viability assay and cell cycle changes after culture of DG75-AB7 in the absence (−) or presence of doxycycline (*Dox*). Cells were stained with propidium iodide, and cell cycle analysis was carried out with FlowJo Software. *C*, Western blot demonstrating changes in expression of the BCL6 target gene, ATR on culture of DG75-AB7 with doxycycline (*Do*). DNA repair capacity in DG75-AB7 was repressed by BCL6. Levels of phosphorylated H2AX after x-irradiation in either the absence (*red bars*) or presence (*blue bars*) of doxycycline were determined by flow cytometry ($n = 3$). H2AX levels specifically in G_0/G_1 of the cell cycle are presented. There are significant differences in levels of phosphorylated H2AX (Mann-Whitney *U* test) at 1 Gy ($p = 0.003$), 2 Gy ($p = 0.007$), and 4 Gy ($p = 0.01$). *, $p < 0.05$, **, $p < 0.01$.

to the mRNA expression of these genes showed ≥30% induction of expression in 14/19 (73%) on the addition of doxycycline (Table 3A). In an alternative method to validate the gene expression changes observed in DG75-AB7, we utilized published data, which in another Burkitt lymphoma cell line has demonstrated a set of genes that bind BCL6 at their genomic loci (34). 39 of the 44 genes that bound BCL6 by ChIP-quantitative PCR are represented on the gene expression microarrays we employed, and 18 (46%) of these showed altered mRNA expression (≥30% induction or repression) at one or more time points after the addition of doxycycline to DG75-AB7 (Table 3B). Although not all genes discovered through ChIP-chip will be functionally important, our data support a functional role for several *e.g.* TNFAIP8, TAP1, SUB1, and CD53, that have not yet been investigated in detail.

One of the important effects of BCL6 is suppression of DNA damage responses partly through transcriptional repression of ATR (23). To show that DG75-AB7 reproduces this aspect of BCL6 deficiency, DNA damage responses in response to x-irradiation were determined. Culture in doxycycline caused induction of ATR protein in AB7 and significant (Mann-Whitney *U* test) reductions in DNA damage in response to x-irradiation (as determined by H2AX phosphorylation) at 1 Gy ($p = 0.003$), 2 Gy ($p = 0.007$), and 4 Gy ($p = 0.01$) (Fig. 2*C*). Therefore, DG75-AB7 is a model system demonstrating gene expression and functional changes on the addition of doxycycline, in line with known BCL6 effects.

The JAK2 Inhibitor, Lestaurtinib, Reveals a Survival Pathway in BCL6-deficient Cells—We utilized a drug sensitivity screen to determine survival pathways in BCL6-deficient DG75-AB7. The effect of each compound in the library on cell viability was

TABLE 1

Genes, whose expression altered ≤0.5-fold or ≥2-fold at one or more time-points after the addition of doxycycline

F-Fold change in expression compared to baseline conditions is presented at 16, 48, and 96 h. For several genes, *e.g.* CCL3L1 and TAP1, multiple probes are present on the Affymetrix chip, and all data are presented in the table. Conditional formatting is employed such that induced gene expression is colored red, and repressed expression is colored blue.

Time (Hours)			Gene Symbol	Transcript Cluster ID
16	48	96		
2.5	4.6	31.8	IFI44L	7902541
1.2	1.7	11.4	IFI27	7976443
5.5	5.6	10.2	CYSLTR1	8173745
2.3	5.8	8.6	LAPTM5	7914270
1.9	2.1	5.4	OAS2	7958913
2.1	3.0	5.0	IFI44	7902553
1.9	2.4	4.7	XAF1	8004184
1.5	2.5	4.7	SP140	8048898
3.0	3.0	4.1	EVI2A|EVI2B	8014066
2.3	2.4	3.7	PARP9	8090018
2.1	2.4	3.6	SP110	8059650
2.6	2.9	3.6	PDCD4	7930454
3.2	2.7	3.6	CXorf21	8171896
2.1	2.7	3.6	SAMD9L	8140971
1.3	1.5	3.6	IFITM1	7937335
2.7	2.7	3.6	SESN1	8128698
3.1	3.6	3.6	C13orf18|LOC7	7971486
1.3	1.6	3.5	FAIM3	7923917
1.8	2.6	3.5	CCL3L1|CCL3L	8019731
1.8	2.6	3.5	CCL3L1|CCL3L	8014414
1.8	2.6	3.5	CCL3L1|CCL3L	8014391
1.0	1.4	3.5		8100758
2.3	2.0	3.4	DDIT4	7928308
1.6	1.9	3.4	OAS1	7958884
2.2	3.2	3.4	TP63	8084766
2.8	2.5	3.3	FLI1|EWSR1	7945132
1.4	1.8	3.3	EBI2	7972557
2.0	1.9	3.3	C18orf17	8020630
2.4	2.7	3.2	BCL2A1	7990818
1.5	2.3	3.1	HIST1H2BK	8124492
2.4	2.3	3.1	GAB1	8097586
1.8	2.5	3.0	ARHGEF3	8088247
2.0	2.5	3.0	RNF213	8010454
2.4	2.5	3.0	IKZF1	8132819
1.5	1.9	3.0	STAT1	8057744
1.9	2.1	3.0	DTX3L	8082075
2.0	2.0	3.0	GCET2	8089478
2.0	2.3	2.9	KIAA1618	8010426
1.9	2.5	2.9	DNMBP	7935660
1.2	1.7	2.9	IFIT3	7929052
2.1	2.4	2.8	TP53INP1	8151890
1.1	1.8	2.8	S100A10	7920123
1.0	1.7	2.8	CCR7	8015031
1.6	2.1	2.7	CCL3	8014369
2.1	2.3	2.7	REPIN1	8137225
2.2	2.5	2.7	SYK	8156321
2.7	2.6	2.7	GPR174	8168531
2.2	2.2	2.7	FUT8	7975136
1.3	1.7	2.7	LGALS9|LOC6	8005458
2.6	2.1	2.6	HIVEP2	8129953
1.3	1.4	2.6	TNFSF8	8163629
1.2	1.7	2.6	LGALS9|LOC2	8013450
1.6	1.9	2.6	PLEK	8042391
2.3	2.3	2.6	MAML3	8102862
1.7	1.9	2.6	KLRK1|KLRC4	7961151
1.2	1.9	2.6	IFIT2	7929047
1.5	2.0	2.6	IFIT1	7929065
1.7	2.0	2.6	SMAP2	7900426
1.9	2.0	2.5	UTRN	8122464
1.6	2.1	2.5	MLKL	8002778
2.4	1.7	2.5	IKZF2	8058670
2.0	2.1	2.5	MEIS2	7987385
2.3	2.4	2.5	CAMK4	8107307
1.3	1.4	2.5	IFI6	7914127
1.9	1.7	2.5	UGCG	8157216
1.3	1.8	2.4	PIK3IP1	8075483
1.4	2.2	2.4	C10orf64|WDF	7927405
2.3	2.3	2.4	7A5	8138466
3.1	2.0	2.4	ID3	7913655
1.8	2.0	2.4	LMO4	7902810
2.5	2.3	2.4	ARHGAP15	8045563
1.6	1.9	2.4	ITPR2	7961900
1.4	1.6	2.4	PML	7984779
1.4	2.0	2.4	WDFY4|C10orf	7927425
1.6	2.2	2.4	RAPGEF1	8164665
2.3	1.8	2.4	RB1	7969017
1.6	1.9	2.4	BLNK	7935270
2.1	2.3	2.4	KLRC4|KLRK1	7961166
2.1	2.1	2.3	BCL11A	8052399
2.3	2.1	2.3	ANKRD44	8057990
2.7	2.2	2.3	LRRN3	8135488
2.4	2.1	2.3	SESN3	7951077
1.8	2.0	2.3	BTN3A2	8117435
1.6	1.8	2.3	BTN3A3	8117476
2.0	1.9	2.3	TBCEL	7944623
2.0	1.7	2.3	CD180	8112428
1.3	1.5	2.3	ENPP3	8122071
1.4	1.7	2.3	PNRC1	8121076
1.7	1.6	2.3	IFIH1	8056285
1.6	1.8	2.3	CASP1	7951397
1.6	1.9	2.3	IGF2R	8123181
1.8	1.8	2.3	ATM|NPAT	7943620
2.2	2.3	2.3	MLLT3	8160332
1.5	1.8	2.3	ST6GAL1	8084717
1.4	1.8	2.2	CD48	7921667
1.2	1.5	2.2	CD72	8161004
1.2	1.1	2.2		8083592
2.4	2.1	2.2	MEF2C	8113039
1.7	1.8	2.2	PTPN6	7953569
1.8	1.7	2.2	SAMD9	8140967
1.5	2.0	2.2	PSCD1	8018922
2.1	2.3	2.2	CHML	7925500
1.8	1.9	2.2	IGF2BP3	8138566
1.3	1.6	2.2	LRRC33	8084951
1.8	1.9	2.2	MGAT5	8045349
1.5	1.9	2.2	IFI35	8007446

Time (Hours)			Gene Symbol	Transcript Cluster ID
16	48	96		
1.8	1.9	2.2	IGJ	8100827
2.1	1.9	2.2	AIM1	8121277
1.4	1.6	2.2	CNR2	7913705
1.9	1.9	2.1	DZIP3	8081503
1.9	2.0	2.1		8043429
1.9	2.0	2.1		8053720
1.6	1.6	2.1	PTK2B	8145490
1.7	1.7	2.1	FOXP1	8088776
1.7	1.9	2.1	HERC2P4	8001099
1.3	1.5	2.1	BST2	8035304
1.9	2.0	2.1	PRDM15	8070503
1.6	1.8	2.1		7947421
1.2	2.1	2.1	ACSM3	7993756
1.5	1.7	2.1	DGKD	8049317
1.3	1.4	2.1	TAGAP	8130539
1.8	1.7	2.1	SLC44A5	7917052
2.0	1.8	2.1	CTDSP2	7964579
1.8	1.7	2.1	PCMTD1	8150714
1.2	1.5	2.1	RPS29	7978824
1.2	1.7	2.1	VSTM3	8081799
1.5	1.7	2.1	OXR1	8147848
2.3	1.7	2.1	PSCDBP	8055980
2.0	1.7	2.1	RCSD1	7907079
2.2	2.1	2.1	SCN3A	8056376
1.5	1.6	2.1	FNBP1	8164607
2.2	1.7	2.1	CDKN1B	7954029
1.6	1.5	2.1	EIF2AK2	8051501
1.8	1.8	2.1	IFI16	7906400
2.1	2.2	2.1	TMEM154	8103226
1.6	1.9	2.1	HERC2P4	8001067
1.3	1.6	2.1	IRF9	7973618
1.7	1.7	2.1	BMI1	7926609
1.8	1.8	2.1	MCTP2	7986293
1.6	1.9	2.1	ERAP2	8107044
2.0	1.9	2.1	ITPR1	8077376
2.0	2.1	2.1	SNTB1	8152606
1.9	1.6	2.1	C5orf13	8113504
1.4	1.8	2.1	TRIM22	7938035
1.6	1.6	2.0	STAT2	7964119
1.8	2.0	2.0	ABCA1	8162940
1.8	2.0	2.0	PLXNC1	7957570
1.5	1.7	2.0	DDX58	8160559
1.8	2.0	2.0	BTN3A1	8117458
1.6	1.7	2.0	HERC2P2|LOC	7986701
1.6	1.8	2.0	LOC283755|HE	7986569
2.1	2.0	2.0	EIF2AK3	8053668
1.7	2.1	2.0	IL10RA	7944152
1.8	1.7	2.0	HEG1	8090193
1.6	1.7	2.0	HERC2P2|LOC	7982154
1.6	1.7	2.0	TAP1	8178867
1.6	1.7	2.0	TAP1	8180061
1.9	1.5	2.0	PLSCR1	8091327
1.6	1.7	2.0	TAP1	8125512
1.8	1.4	2.0	MAPK10	8101587
2.6	2.4	2.0	RASSF6	8100943
1.5	2.0	2.0	RP5-1022P6.2	8064868
1.2	2.0	1.9	FLJ31958	7933638
2.1	1.2	1.9	MGC16169	8102171
2.0	1.8	1.9	CDC2L6	8128867
0.5	0.4	1.9		8058340
1.6	2.1	1.8	KBTBD8	8080911
2.2	1.7	1.8		8101699
2.0	1.6	1.8	FRYL	8100251
2.3	2.2	1.7	LOC389765	8156164
2.1	1.4	1.6	PTPRC	7908553
2.3	1.9	1.6	SLC30A4	7988426
2.8	1.7	1.6	GPRIN3	8101757
2.1	1.6	1.6	RCN2	7985089
2.2	1.6	1.5	NEK7	7908543
2.0	1.6	1.3	STAMBPL1	7929012
0.4	0.9	0.9	ALDOC	8013660
0.5	0.5	0.6		8136159
0.4	0.6	0.6		8109424
0.4	0.5	0.5	HMGCS1	8111941
0.5	0.5	0.5	PMEPA1	8067233
0.7	0.6	0.5	LYAR	8099107
0.7	0.8	0.5		8151709
0.8	0.8	0.5	LOC85389	7952339
0.8	0.6	0.5	ATP2A2	7958644
0.7	0.5	0.5	CDC6	8007071
0.7	0.6	0.5	E2F8	7947110
0.5	0.7	0.5	SERPINA9	7981084
0.7	0.6	0.5	TIPIN	7989915
0.7	0.5	0.5	CDC25A	8086880
0.6	0.7	0.5	SNORD75	7922416
1.2	0.8	0.5	MAP1A	7983228
0.7	0.6	0.5	TUBB2C	8159642
0.5	0.7	0.5	RPL27A	7938295
0.6	0.6	0.5	MRTO4	7898549
1.0	0.6	0.5	SLC1A4	8042310
0.5	0.6	0.5	LGMN	7980958
0.6	0.5	0.5	SFRS6	8062695
0.9	0.7	0.4	PSAT1	8156043
0.8	0.6	0.4	C11orf53	7943729
0.6	0.6	0.4	TFRC	8093053
1.0	0.7	0.4	CCPG1	7989037
0.8	0.7	0.4	SNORD50B	8127989
0.7	0.6	0.4		8001529
0.4	0.4	0.4		8047555
0.5	0.5	0.4	HSPA5	8164165
0.4	0.4	0.4		8047557
1.1	0.7	0.4	CHAC1	7982868
0.8	0.9	0.4	LOC85391	7952335
1.0	0.6	0.4	CTH	7902290
0.4	0.5	0.3		8059648
0.9	0.5	0.3	SLC7A11	8102800

estimated both in the presence and absence of doxycycline. In each case the effect was quantified as a z-score, with negative z-scores representing inhibition of cell survival (Fig. 4*A*). As expected, the majority of compounds do not show an effect on cell survival, but comparison of z-score data from DG75-AB7 cell screens in the presence of doxycycline (BCL6 deficient) or absence of doxycycline (BCL6 replete) allowed identification of compounds that preferentially reduced survival of BCL6-deficient cells while having relatively little effect on BCL6 replete cells (Table 4). Seven compounds demonstrated z-scores ≤−2 at two or more concentrations. Of these compounds, paclitaxel and vinorelbine reduced survival of both BCL6 replete and deficient cells, whereas others, 2-methoxyestradiol, dasatinib, canertinib, lestaurtinib, and sunitinib appeared to preferentially suppress growth of BCL6 deficient cells (Fig. 4*B*). By comparison doxorubicin and flavopiridol (Fig. 4*C*) reduced survival without a differential effect on BCL6-deficient cells, whereas cyclophosphamide and olaparib showed no effect on either BCL6 replete or deficient cells.

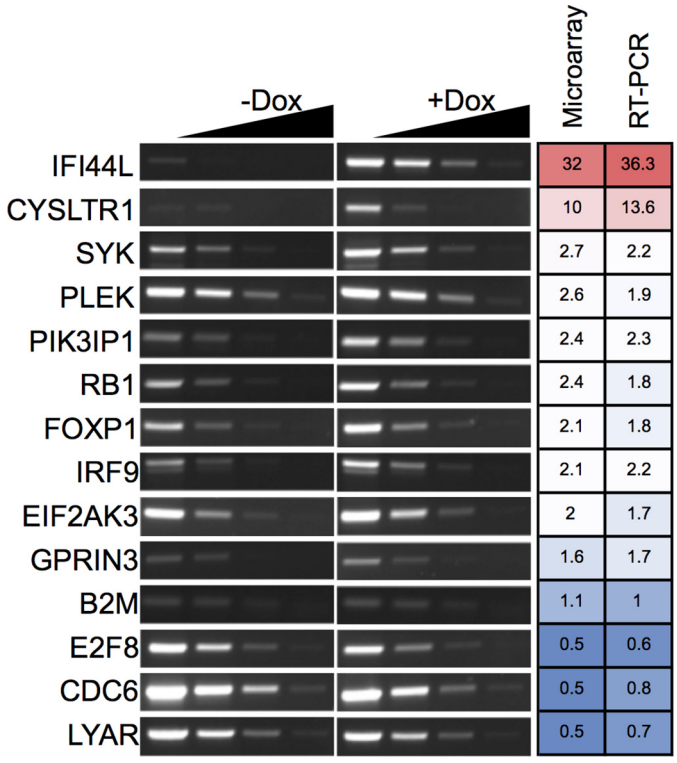

FIGURE 3. **Validation of microarray results by RT-PCR of 14 selected genes.** Primer sequences are presented in Table 2. RT-PCR was carried out from cDNA produced from DG75-AB7 cultured in the presence (+*Dox*) or absence (−*Dox*) of doxycycline (1 μg/ml) for 96 h. cDNA dilutions of 1, 1:5, 1:25, and 1:125 (*left to right* as indicated by the *black triangles*) were prepared and used as the template for the PCR. *Columns to the right* show the -fold induction obtained for each gene from the microarray results and the corresponding inductions calculated from the RT-PCR. Conditional formatting indicates induced genes (*red*) and repressed genes (*blue*) (Microsoft Excel v14.4.7).

BCL6 Deficiency Induces a Transcriptional Increase in JAK2 Levels—We focused further work on the JAK2 inhibitor, lestaurtinib, because BCL6 directly represses STAT3 (7), which is a principle target of phosphorylation by JAK2, and we wondered whether BCL6 also repressed JAK2 to cause increased overall inhibition of JAK2 and STAT3. The addition of doxycycline caused a 4-fold increase in JAK2 mRNA and induction of JAK2 protein (Fig. 5, *A* and *B*). Induction of phosphotyrosine 705-STAT3 accompanied these changes, and lestaurtinib and two other JAK2 inhibitors, fedratinib and ruxolitinib, prevented phosphorylation (Fig. 5*C*). At the doses employed, ruxolitinib and to a lesser extent fedratinib, stabilized JAK2 phosphorylation (in line with their mechanism of action as type I inhibitors (35)), whereas all three agents repressed STAT3 phosphorylation. STAT3 transcription factor activity is largely associated with phosphorylation on tyrosine 705. Westerns blots, utilizing tyrosine 705- and serine 727-specific anti-phospho-STAT3 showed STAT3 tyrosine 705 after induction of BCL6 deficiency, whereas levels of phosphorylated STAT3 serine 727 remain unchanged (Fig. 5*D*). Overall, the data demonstrated preferential reduction of survival of BCL6-deficient DG75-AB7 by lestaurtinib, and consistent with this effect being mediated by STAT3, JAK2 inhibitors repressed the STAT3 phosphorylation induced by BCL6 deficiency.

In order to confirm that the reduction in viability observed with lestaurtinib was mediated through JAK2 we transfected DG75-AB7 either with siRNA directed against JAK2 or a negative control siRNA (Fig. 5, *E* and *F*). Repression of JAK2 caused a significant (*t* test; $p = 0.008$) reduction in cell viability in the presence of doxycycline.

BCL6 Deficiency Induces IL10RA Expression—Serum IL-10 levels are prognostic in DLBCL (36), and IL10 receptor expression was increased in ABC-DLBCL as compared with germinal

TABLE 2
Primer sequences for RT-PCR presented in Fig. 3

Gene	Primers (5′ to 3′) Forward	Reverse	Product size
			bp
IFI44L	tggccaagccgtagtggggt	cccgcagcatctgcctcagtg	605
CYSLTR1	tgtgccctgctctctcccct	ggtgctgaggcggcacaaga	658
SYK	cggctggagagcgaggagga	ggcccagtcttgggctgcac	462
PLEK	tgaccctgctggggcagaaga	acccctgggctgtttcccgt	325
PIK3IP1	tctgggctacgtgctgggca	ctcagcccacagggccacct	456
RB1	ccggaggacctgcctctcgt	cctcgcctgggtgttcgagg	653
FOXP1	cgggcggcagcaaccactta	ggctgcccgggctgaattgt	577
IRF9	agagatcagccgcccagcca	gcaacatccatgcggcccct	390
EIF2AK3	ctgcggccgaggtgactgtg	ccactgcgaggtccgacagc	562
GPRIN3	gatgggtacaccccgggcct	gggaggggagcgcagtcaga	415
B2M	agatatgcctgccgtgtg	aatccaaatgcggcatct	110
E2F8	gtgcgctcagctgggacctg	gctgtcggtgtccacggctc	350
CDC6	gggtgaaggctgcgggttcc	ccctttccctggcaggcagc	578
LYAR	ggcgctggctgagaggcaat	cccctgctgttccacggcg	669

TABLE 3

Transcriptional regulation of genes after the addition of doxycycline to DG75-AB7

F-Fold induction of mRNA levels at 16, 48, and 96 h after doxycycline treatment are shown. Individual values are color-coded utilizing a conditional formatting tool (Microsoft Excel v14.4.7) with the scale being from red (the highest value) to white (the lowest value). BCL6 target genes were defined by two alternative approaches. A) genes determined experimentally to be functional BCL6 targets18, and B) set of genes for which BCL6 binding to the gene locus has been experimentally ascertained by ChIP-chip (34). In both tables genes are ordered such that the least transcribed (defined by normalized Affymetrix values) is at the top and the most transcribed is at the bottom. Only CCL3 is present in both tables.

A

Gene	Time (Hours)			Reference
	16	48	96	
PRDM1	1	1	1.1	Shaffer et al. 2000, Tunyaplin et al. 2004
IFITM3	1.1	1	1	Shaffer et al. 2000
CD44	1	1	1	Shaffer et al. 2000
EBI2	1.4	1.8	3.3	Shaffer et al. 2000
CCND2	1	1	1	Shaffer et al. 2000
CD69	1.2	1.2	1.3	Shaffer et al. 2000
CCL3	1.6	2.1	2.7	Shaffer et al. 2000
STAT2	1.6	1.6	2	Shaffer et al. 2000
CDKN1B	2.2	1.7	2.1	Shaffer et al. 2000
ID2	1.9	1.2	1.6	Shaffer et al. 2000
ATR	1.4	1.4	1.2	Ranuncolo et al. 2007
BCL2L1	0.9	0.9	1	Tang et al. 2002
IFITM1	1.3	1.5	3.6	Shaffer et al. 2000
CD80	1.5	1.5	1.6	Niu et al. 2003
STAT3	1.2	1.3	1.4	Ding et al. 2008
STAT1	1.5	1.9	3	Shaffer et al. 2000
TP53	1	1.1	1.3	Phan et al. 2004
NFKB1	1.4	1.3	1.4	Li et al. 2005
CXCR4	1.3	0.9	1.2	Shaffer et al. 2000

B

Gene	Time (Hours)		
	16	48	96
ZNF443	1.4	1	1
HELB	1.2	1.4	1.4
CCL3	1.6	2.1	2.7
TNFAIP8	1.6	1.5	1.8
BMPR2	1.5	1.4	1.5
BRPF1	0.9	0.8	0.7
HIST1H4E	1	0.8	0.9
TAP1	1.6	1.7	2
MYST4	1.3	1.2	1.2
RHOH	1.4	1	1
SLC39A8	0.7	0.7	0.7
SUB1	1.6	1.7	1.6
CDC20	1	0.6	0.8
CHEK1	0.9	0.7	0.7
CD74	1	1.2	1.5
TARS	1.3	1.1	1
CD53	1.4	1.4	1.7
TEGT	0.9	0.9	0.7

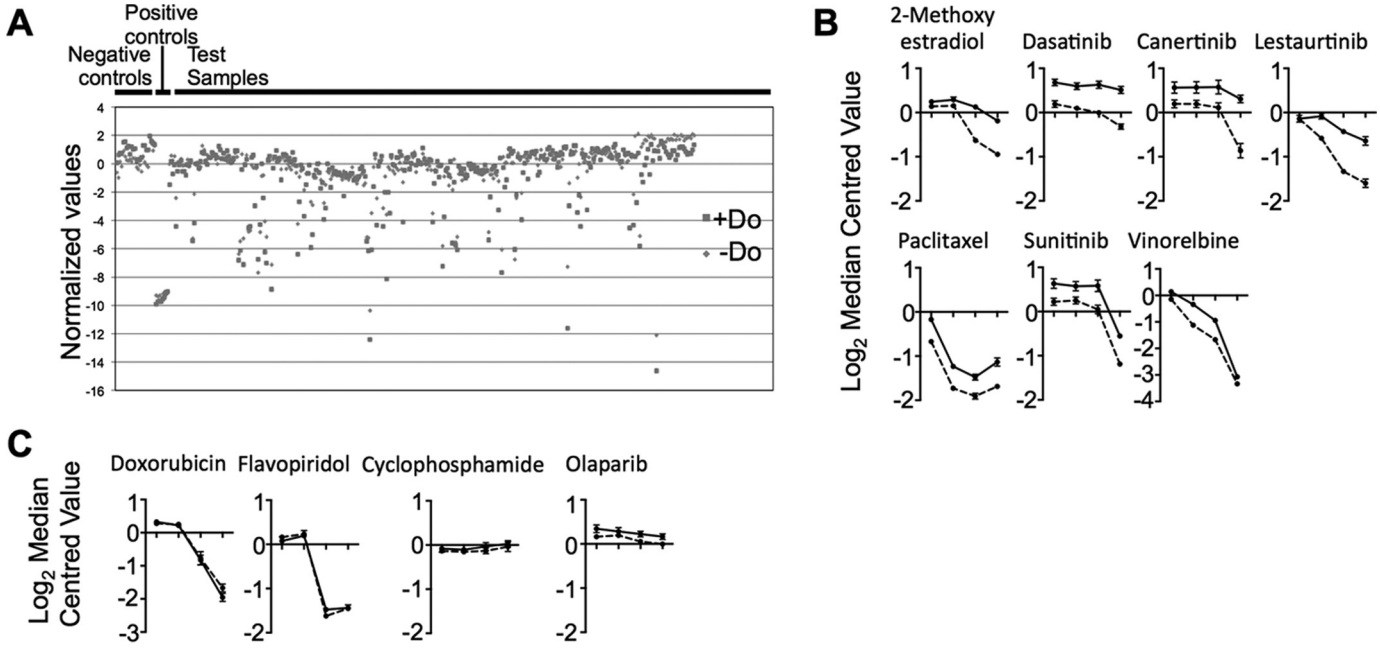

FIGURE 4. **Small molecule inhibitor screen for enhanced loss of viability in BCL6-deficient DG75-AB7.** *A*, overview of the screen. Standardized values (drug effect z-score), calculated from x ($\log_2$ median raw value), μ ($\log_2$ median plate raw values), and σ (S.D of differences between $\log_2$ raw values in the presence and absence of doxycycline (*Do*)) according to the formula z-score $= (\times - \mu)/\sigma$ are plotted for negative controls (DG75-AB7 cells in the absence or presence of doxycycline but without any of the screening agents) and positive controls (DG75-AB7 cells in the absence or presence of doxycycline and with the potent kinase inhibitor, staurosporine (10 μM), to induce apoptosis). For the test samples, standardized values for each agent and at each concentration are shown. *B*, effect of agents with z-scores ≤ -2 (Table 4) on cell survival determined by ATP luminescence. Survival of cells without doxycycline (*solid line*) or with this agent (*dotted line*) at four concentrations (1, 10, and 100 nM and 1 μM) is shown. Lestaurtinib was employed at 0.2, 2, 20, and 200 nM. *C*, by contrast, doxorubicin and flavopiridol reduce survival of both BCL6 replete and deficient DG75-AB7 cells, whereas cyclophosphamide and olaparib have no effect on survival.

TABLE 4

Small molecule inhibitor screen

Compounds at concentrations from 1, 10, 100, and 1000 nM were administered to DG75-AB7 in the presence or absence of doxycycline, and the surviving fraction was measured. Drug-effect z-scores were calculated. Standardized value (drug effect z-score) is calculated from x ($\log_2$ median raw value without doxycycline $-\log_2$ median raw value with doxycycline), μ ($\log_2$ median plate raw values), and σ (S.D. of differences between $\log_2$ raw values in the presence and absence of doxycycline) according to the formula z-score = $(x - \mu)/\sigma$. z-scores of −2 or less at two or more concentrations were obtained for 2-methoxyestraduiol, dasatinib, canertinib, lestaurtinib, paclitaxel, and sunitinib (indicated by the brown bar to right of table). z-scores of −2 or less at one concentration-only were obtained for a further group of compounds (blue bar to right of table), and compounds for which no significant z-scores were obtained are indicated by the orange bar to right of table. Individual z-scores were color-coded utilizing a conditional formatting tool (Microsoft Excel v14.4.7) with red indicating low, white indicating mid-range, and blue indicating high scores.

Compounds	Concentration (nM)			
	1	10	100	1000
2-methoxyestradiol (Anti-angiogenesis)	-0.3	-0.4	-3.0	-3.2
Dasatinib (BCR-ABL/Srci)	-2.2	-2.2	-2.8	-3.9
Canertinib (pan-ErbBi)	-1.9	-2.0	-2.2	-4.7
Lestaurtinib (JAK2/FLT3/TrkAi)	0.7	-2.2	-2.3	-3.9
Paclitaxel (Microtubule inhibitor)	-2.2	-2.1	-1.5	-2.1
Sunitinib (VEGFR1-3i,PDGFRi,Kiti,CSF1Ri)	-1.8	-1.2	-2.4	-2.6
Vinorelbine (Anti-mitotic)	-0.8	-3.6	-2.9	-0.9
17-AAG (HSP90i)	-1.9	-1.3	-2.9	0.0
Lapatinib (Her2i)	0.8	0.2	-2.0	1.4
PD-0332991 (CDK4/6i)	0.4	0.3	-0.9	-2.2
PF-00299804 (pan-ErbBi)	-0.2	0.5	0.2	-4.1
Salinomycin (Microtubule inhibitor)	0.0	-0.1	-1.9	-4.6
Curcumin (NSAID)	-1.1	-1.3	-1.3	-3.9
MK-1175 (WEE1i)	0.6	-0.1	-3.7	-0.8
PF-03814735(Aurora kinase i)	0.7	0.3	-0.6	-3.6
PF-02341066 (MET/ALKi)	-1.9	-1.7	-1.5	-2.6
SAR-20106 (CHK1i)	-0.1	0.0	-0.1	-2.5
Everolimus (mTORi)	-1.3	-0.9	-1.7	-2.3
PF-04691502 (PI3K/mTORi)	0.2	0.1	-1.6	-2.2
6-thioguanine (Anti-metabolite)	0.6	-0.3	-0.6	-2.4
PF-03758309 (PAKi)	-2.0	0.1	-0.3	0.8
Sutent (VEGFR1-3i,PDGFRi,Kiti,CSF1Ri)	0.0	-0.1	-0.9	-2.3
BIBW2992 (EGFR/HER2i)	0.2	0.0	0.0	-2.1
PF-00477736 (CHK1i)	1.0	-0.2	-2.4	0.8
Bleomycin sulfate (Chemotherapy)	-1.5	-1.1	-1.7	-1.9
Camptothecin (TOPOIi)	-1.8	-1.9	-0.7	-1.2
PLX-4720 (BRAFi)	-1.3	-1.9	-0.2	-1.5
Flavopiridol (CDKi)	1.4	1.1	-0.3	0.6
Olaparib (PARP1/2i)	-0.4	0.0	-0.2	-0.3
Doxorubicin (DNA intercalator)	0.5	0.8	0.8	2.3
Cyclophosphamide (DNA alkylator)	0.2	0.3	0.3	0.7
5-FU (Anti-metabolite)	-0.5	-0.8	-0.6	-2.0
GSK-2334470A (PDKi)	-1.0	-0.1	-0.9	-1.3
Nilotinib (BCR-ABLi)	0.7	0.4	-0.6	-0.5
KU-59652 (ATMi)	0.8	-0.1	-0.5	-1.0
AG-14699 (PfizerPARPi)	0.0	-0.1	0.1	0.2
Indomethacin (NSAID)	0.3	0.0	-0.2	0.0
GDC-0449 (SMOi)	0.2	0.1	0.6	0.2
Carboplatin (DNA cross-linking agent)	0.4	-0.3	0.5	0.1
BI-2536 (PLKi)	-0.9	-1.0	0.2	0.6
4-OH-tamoxifen (ERi)	1.1	0.0	-1.5	-1.6
MK-4827 (PARPi)	0.2	-0.3	-0.5	0.0
Gemcitabine (Pyrimidine analogue)	0.3	-0.9	1.3	1.3
OL-PIX-A17A (LeadTh,PARPi)	1.4	0.6	1.3	0.8
PF-04929113 (HSP90i)	1.3	1.0	1.7	2.7
Imatinib mesylate (BCR-ABLi)	0.6	0.1	1.0	0.2
MK-2512 (PARPi)	0.6	-0.1	0.9	0.4
OL-PIX-F3-B (LeadTh,PARPi)	-0.5	0.5	-0.9	0.7
GSK2194069A (FASi)	0.1	0.1	0.1	-0.6
PF-332991 (CDK4/6i)	0.3	0.7	-2.0	-1.0
Piroxicam (NSAID)	0.8	0.9	0.5	0.8
AZ4547 (FGFRi)	0.9	1.7	0.9	-0.6
Erlotinib (EGFRi)	0.4	0.4	0.3	-1.9
ABT-737 (Bcl2i)	-0.4	0.2	0.3	0.0
BEZ-235 (PI3K/mTORi)	0.4	0.8	-1.3	-1.1
Resveratrol (NSAID)	0.8	0.2	1.0	0.8
XAV-939 (TNKSi/Wnti)	1.0	0.7	1.4	1.1
Decitabine (DNA methylation)	0.2	-0.3	-1.2	-0.2
Sorafenib (Inhibits RAF, PDGF, VEGF1/2)	0.7	0.3	0.5	0.0
Gefitinib (EGFRi)	0.4	0.1	0.2	-1.0
Celecoxib (COX2i)	0.1	0.4	0.6	0.3
Etoposide (TOPOIIi)	1.3	0.2	1.8	1.2
Temozolomide (DNAalkylator)	1.3	0.6	0.4	0.9
GSK1904529A (IGFRi)	0.6	0.8	0.8	0.9
Nutlin3 (MDM2i)	0.0	-0.8	0.2	-0.8
BSI-201 (Sanofi, PARPi)	0.2	-0.6	1.1	1.0
PBS-1086 (NFkBi)	0.8	0.0	0.3	-0.4
CT241533 (CHK2i)	0.6	-0.5	0.5	-0.8
PD173074 (FGFRi)	0.5	1.5	-0.1	-1.8
Voronostat (Class 1/2 HDACi)	0.7	0.1	-1.1	-1.0
MDV-3100 (CRPCi)	-0.5	-0.2	0.1	-0.3
EB-47 (PARPi)	0.4	-0.2	-0.2	-0.5
PRIMA1 (Mut-p53 activator)	0.6	0.3	0.4	0.7
PBS-1169 (NFkBi)	0.1	0.3	0.6	0.4
KU0057788 (DNA-Pki)	0.1	-0.2	0.4	-1.6
PD-184352 (MEKi)	0.7	0.8	0.4	0.3
Sapacitabine (CNDAC)	-0.3	0.0	0.1	0.8

center (GC)-DLBCL (29). IL10 receptor activation promoted STAT3 phosphorylation and DLBCL survival (29). We wondered whether JAK2/STAT3 phosphorylation required IL10 receptor expression and engagement in DG75-AB7. Induction of BCL6 deficiency induced IL10RA mRNA expression (Fig. 5*G*), and flow cytometry showed elevated surface expression of IL10RA in a population of DG75-AB7 cells (Fig. 5*H*). It is not clear why IL10RA expression was not induced in all cells. Exogenous IL10 induced STAT3 tyrosine phosphorylation, which is repressed by a blocking anti-IL10 antibody (Fig. 5*I*), demonstrating that IL10RA engagement is required for STAT3 phosphorylation. Collectively, our data implicates BCL6 in suppressing an IL10RA/JAK2/STAT3 pathway.

Lestaurtinib Combined with Induced BCL6 Deficiency Is Effective in a Mouse Xenograft Model—To evaluate *in vivo* efficacy of lestaurtinib in combination with BCL6 deficiency, we utilized SCID-beige mouse xenografts. Animals were flank-injected with DG75-AB7 and divided into four groups ($n = 8$). Although there were no obvious histological differences between tumors in untreated animals and those that had received either doxycycline in the drinking water or lestaurtinib by intraperitoneal injection (Fig. 6), those tumors from animals that received both agents unexpectedly showed massive central necrosis. As compared with untreated animals, mice that received either doxycycline or lestaurtinib alone showed reduced growth, and the combination of agents produced further repression (Fig. 6*C*). Immunohistochemical assessment of proliferation demonstrated that the combination of doxycycline and lestaurtinib increased the fraction of non-proliferating Ki-67 negative cells (Fig. 6*D*). Therefore, BCL6 deficiency was sufficient to markedly repress tumor growth without altering the fraction of Ki-67-expressing cells, but the combination of BCL6 deficiency and lestaurtinib significantly (Mann-Whitney *U* test; $p = 0.007$) increased numbers of Ki-67-negative cells and was associated with tumor necrosis.

JAK2 Is a Direct Target of BCL6 Transcriptional Repression—Inspection of the JAK2 promoter region identified a possible BCL6 binding site at −1185 bp from the transcription start site (Fig. 7*A*). To demonstrate BCL6 binding to this sequence *in vitro*, we utilized gel shift assays employing lysates from the BCL6 expressing Ramos Burkitt lymphoma cell line and labeled JAK2 promoter BCL6 binding sequence (J2B6BS) oligonucleotide. A protein-DNA complex was effectively competed by a consensus BCL6 binding sequence (FB20) (7), and an anti-BCL6 antibody caused disappearance of the shifted band (Fig. 7*B*), therefore, identifying the complex as containing BCL6. FB20 oligonucleotide was able to compete more effectively than J2B6BS for binding to BCL6, suggesting a relatively weak interaction at the JAK2 promoter. To show *in vivo* BCL6 binding at the JAK2 promoter, we analyzed publicly available ChIP-seq databases (37). Statistically significant peaks (Table 5) of BCL6 binding corresponded with BCOR co-repressor binding without evidence of SMRT or NCOR binding (Fig. 7, *C* and *D*), supporting both a direct effect of BCL6 and association with BCOR at the JAK2 locus. To demonstrate BCL6 binding at the JAK2 locus in DG75-AB7, a single site ChIP assay was employed and showed ~30-fold more binding in the absence of doxycycline (Fig. 7*E*). Next, reporter assays were carried out in

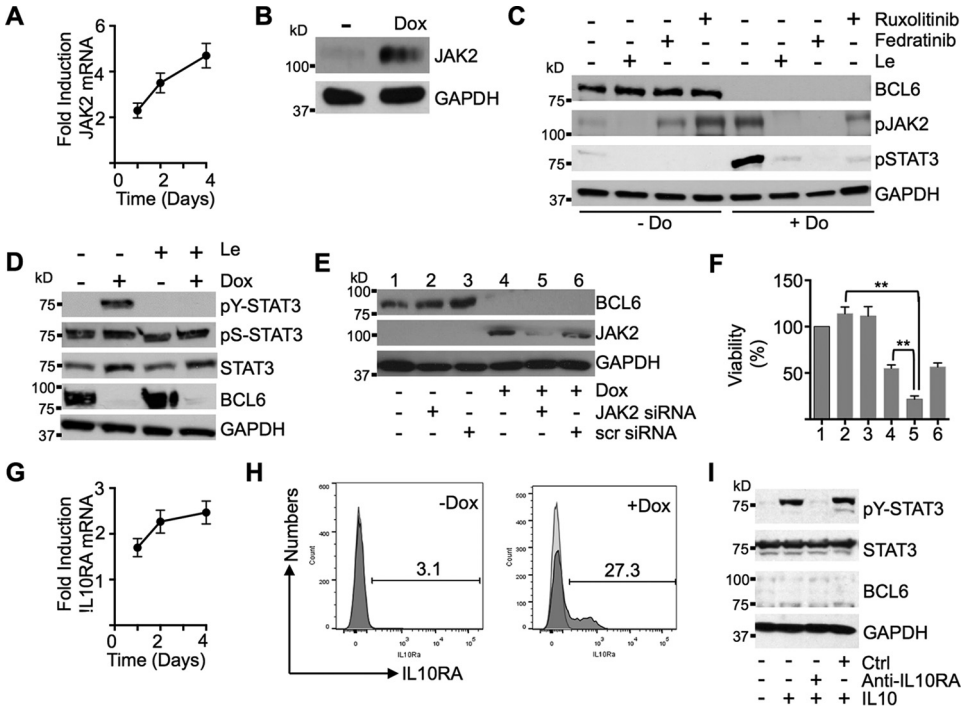

FIGURE 5. **BCL6 deficiency leads to both transcriptional increase in JAK2 and STAT3 phosphorylation.** *A*, mRNA levels of JAK2 determined over 4 days in the presence of doxycycline relative to JAK2 levels in DG75-AB7 cultured without doxycycline. *B*, JAK2 protein levels determined by Western blot in DG75-AB7 after culture for 4 days with doxycycline (*Dox*). *C*, JAK2 inhibitors suppress STAT3 phosphorylation. Western blots showing expression of phosphorylated JAK2 and phosphorylated STAT3 in DG75-AB7 in the absence (−*Dox*) and presence (+*Dox*) of doxycycline (*Do*) and after treatment with lestaurtinib (*Le*; 200 nM), fedratinib (2 μM), and ruxolitinib (200 nM). *D*, specific phosphotyrosine-STAT3 expression. Western blots showing expression of phosphorylated STAT3-tyrosine 705 (*pY-STAT3*), phosphorylated STAT3-serine 727 (*pS-STAT3*), total STAT3, and BCL6 in the presence or absence of doxycycline (*Dox*) or lestaurtinib (*Le*) as indicated. *E*, JAK2 siRNA knockdown. DG75-AB7 were mock-transfected (*lanes 1* and *4*) and transfected with a JAK2 siRNA (*lanes 2* and *5*) or a scrambled (*scr*) negative control siRNA (*lanes 3* and *6*) in the absence (*lanes 1–3*) or presence (*lanes 4–6*) of doxycycline). Cell lysates were harvested 48 h after transfection and 24 h after the addition of doxycycline. *F*, relative viability compared with mock-transfected cells without doxycycline. Column numbers are as in *E* above. *G*, induction of IL10RA mRNA after repression of BCL6 in DG75-AB7. JAK2 siRNA significantly reduces (*t* test, $p = 0.008$) viability in the presence of doxycycline. **, $p < 0.01$. *H*, histograms showing IL10RA expression by flow cytometry on DG75-AB7 in the presence (+*Dox*) or absence (−*Dox*) of doxycycline. *Light gray* indicates isotype control, and *dark gray* indicates anti-IL10RA. *I*, effects of IL-10 and blocking anti-IL-10 antibody on STAT3 phosphorylation. DG75-AB7 was cultured in the presence of doxycycline and IL10 (10 ng/ml) in the presence of either a blocking anti-IL10RA antibody (5 μg/ml) or an isotype control antibody. Western blotting was carried out for pY-STAT3.

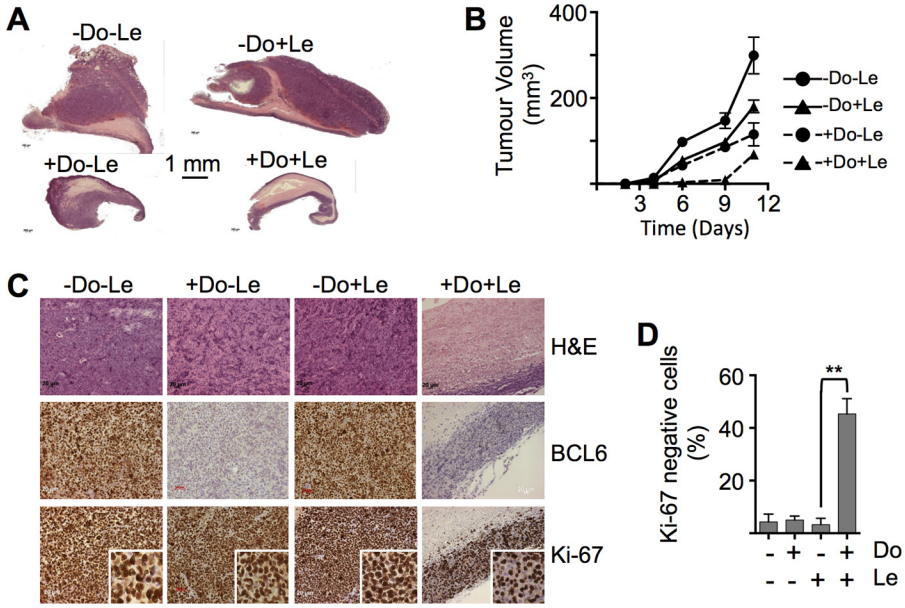

FIGURE 6. **JAK2 inhibition synergizes with BCL6 deficiency to cause tumor necrosis *in vivo*.** *A*, hematoxylin- and eosin-stained sections of representative tumors excised from the flanks of animals receiving neither doxycycline (*Dox*) nor lestaurtinib (−*Do-Le*) either agent alone (+*Do-Le* or −*Do+Le*) or both agents together (+*Do+Le*). Tumors were removed after 12 days of treatment. *B*, histology and immunohistochemistry of tumors from mice treated as indicated with doxycycline (*Dox*) or lestaurtinib (*Le*). The *top row of photomicrographs* shows hematoxylin- and eosin-stained sections. The *middle row* shows sections stained with anti-BCL6, and the *bottom row* demonstrates staining with anti-Ki-67. Insets show higher power views. *C*, increase in tumor volume calculated as described under "Experimental Procedures." Data represent the mean volumes ±S.E. ($n = 8$). *D*, numbers of Ki-67-positive and -negative cells were counted in six high power fields of sections from four mice from each experimental group. Mean percentage (±S.E.) of Ki-67 negative cells is shown.

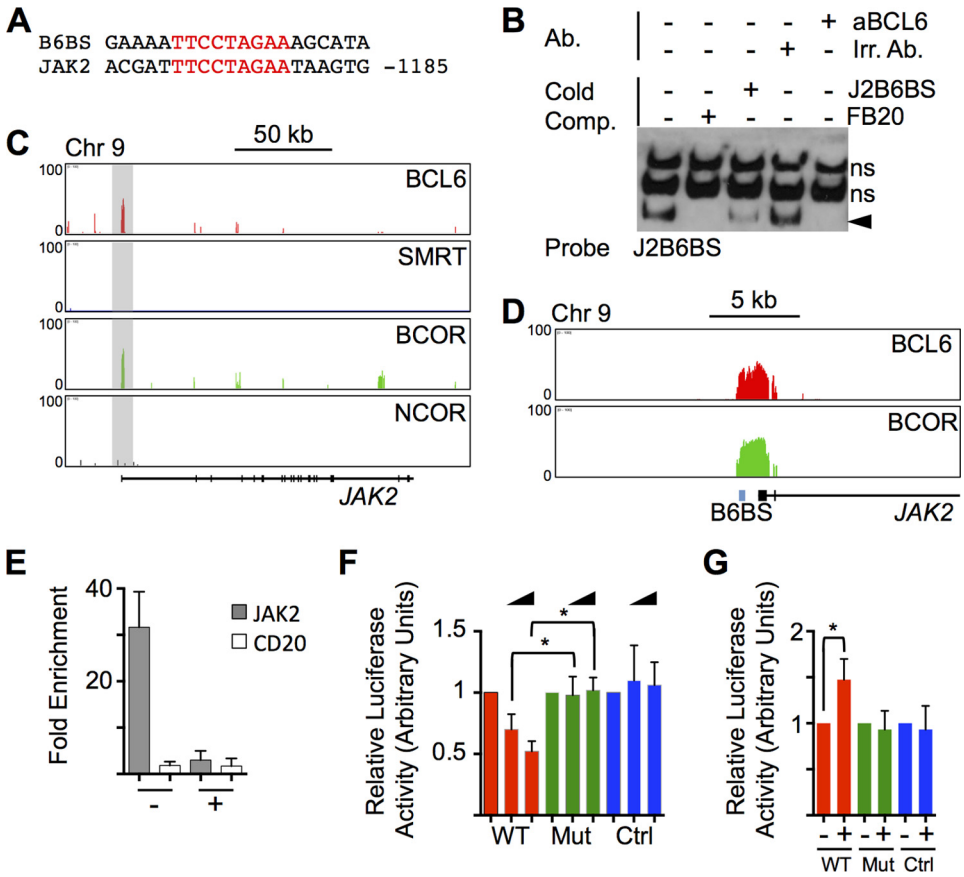

FIGURE 7. **JAK2 is a direct BCL6 target gene.** *A*, BCL6 binding sites in the JAK2 promoter with positions relative to the transcription start site. *B*, *in vitro* binding of BCL6 to the JAK2 BCL6 binding sequence. Gel shift assay were carried out with lysates from DG75-AB7 cells in the absence of doxycycline and labeled JAK2 BCL6 binding sequence oligonucleotide (*J2B6BS*) (50 fmol). The addition of a super-shifting anti-BCL6 antibody (*aBCL6*) caused disappearance of the specific band and formation of the specific BCL6-DNA complex was effectively competed by unlabeled FB20 (a consensus BCL6 binding site 7) and also by J2B6BS. Nonspecific (*ns*) bands that were neither super-shifted nor competed by unlabeled oligonucleotide were observed. *C*, ChIP-seq demonstrating *in vivo* BCL6 binding at the JAK2 locus of the OCI-Ly1 diffuse large B-cell lymphoma cell line employing data from 37. The *gray bar* indicates the peak of BCL6 and BCOR binding at the proximal promoter region. *D*, zoom-in view of the ChIP-seq data to demonstrate the BCL6 binding site (*B6BS*). *E*, single site ChIP assay. ChIP was carried out with anti-BCL6 and anti-actin antibodies followed by real-time PCR for the BCL6 binding site at the JAK2 locus and a site at the CD20 locus, which does not bind BCL6. -Fold enrichment is compared between anti-BCL6 and anti-actin antibodies. *DOX*, doxycycline. *F*, luciferase reporter assays. HEK293 cells were transfected with 0, 50, or 200 ng of a mammalian expression vector bearing full-length BCL6 cDNA (as indicated by the *black triangles*) and luciferase vectors bearing either 2 kb of the proximal JAK2 promoter (*WT*) or this region with mutations of the BCL6 binding site 1 (*Mut*) or a vector bearing a luciferase gene without any inserted promoter sequence (*Ctrl*). Each experiment ($n = 3$) was carried out in triplicate. For WT, Mut, and Ctrl results are normalized to the condition without transfected BCL6 expression vector. There are significant differences (paired *t* test) between mutated and wild-type JAK2 promoter sequences for both 50 ng ($p = 0.015$) and 200 ng ($p = 0.03$) of transfected BCL6 expression plasmid. *, $p < 0.05$. *G*, luciferase reporter assay. DG75-AB7 cells were transfected with luciferase reporter constructs as before. Cells cultured in the presence of doxycycline showed significantly enhanced (paired *t* test; $p = 0.02$) reporter activity. *, $p < 0.05$. ($n = 3$). *Irr. Ab.*, irrelevant antibody.

TABLE 5

Statistical summary of ChIP enrichment data at the JAK2 locus from GEO data, GSE29282 (37)

The statistical test used compares each sample to the reference using a one-tailed binomial test. A false discovery rate of 0.001 was also applied. Partek® Genomics Suite® software version 6.6 (Copyright 2014; Partek Inc., St. Louis, MO) was employed to do the analysis. Absolute signal (read number) and computed significance of enrichment (*p* value) are presented.

	Antibody	
	BCL6	BCOR
Scaled -fold change (ChIP vs INPUT)	33.23	10.8
p value (CHIP vs INPUT)	10^{-45}	10^{-45}
Total reads in region (ChIP)	248	1455
Total reads in region (INPUT)	8	127
Interval length	346	1173
Chromosome	9	9
Start	4,975,124	4,974,600
Stop	4,975,470	4,975,773

HEK293 cells to demonstrate the functional importance of the binding site (Fig. 7*F*). Transcription was repressed from the wild-type promoter, in response to a transfected BCL6 expression vector, and there was relief of repression on mutation of the BCL6 binding site. This result was confirmed in DG75-AB7 (Fig. 7*G*) Therefore, there is a functional BCL6 binding site in the JAK2 proximal promoter region, and BCL6 binds to this region *in vivo*, supporting the direct transcriptional repression of JAK2 by BCL6.

Expression of JAK2 and BCL6 mRNA Are Inversely Correlated in Human DLBCL—To obtain data on relative JAK2 and BCL6 mRNA expression in primary human lymphoma, we analyzed a publicly available gene expression database (38). JAK2 mRNA is expressed significantly more highly in ABC-DLBCL compared with GC-DLBCL (Fig. 8). This adds to previously published data that both STAT3 and IL10RA are found in significantly greater amounts in ABC-DLBCL (7, 29).

Discussion

Burkitt lymphoma cell lines have been useful in determining mechanisms of action and gene targets of BCL6 (18, 39–41).

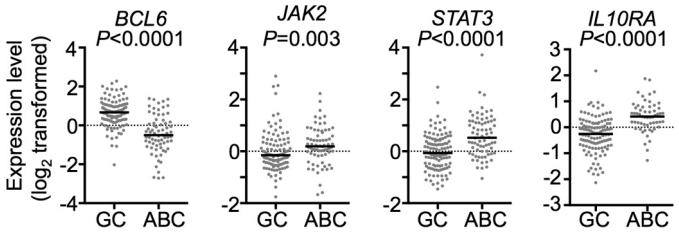

FIGURE 8. **BCL6, JAK2, STAT3, and IL10RA expression levels based on previously published gene expression profiling of cases of diffuse large B-cell lymphoma (50).** The signal values for BCL6 (probe 24429), STAT3 (probe 31469), JAK2 (probe 17330), and IL10RA (probe 34420) were retrieved for 71 ABC-DLBCL and 110 germinal center (*GC*) B-cell-like DLBCL samples. The data had been previously $\log_2$-transformed and median-centered for each gene across the entire sample set. The *p* values are calculated by nonparametric Mann-Whitney (*U* test) to compare the values between the two DLBCL subgroups. *Bars* indicate the group medians.

Both BCL6 (42, 43) and the genes whose transcription it directly inhibits (3, 7, 8) are potential targets for therapy in DLBCL. To produce a model system for the systematic evaluation of BCL6- and BCL6-regulated pathways for therapy, we produced a conditional BCL6-deficient Burkitt lymphoma cell line that reproduces the functional effect of BCL6 on DNA damage responses (23) and many of the gene expression changes known to be due to BCL6. This novel cell line has significant advantages over previous methodologies (18) because minimum perturbation is required to suppress BCL6.

BCL6 deficiency suppressed proliferation of DG75-AB7 and reduced the surviving fraction of cells, but similar to work using a peptide inhibitor to abrogate BCL6 function in a Burkitt lymphoma cell line (44), ~50% of cells remain viable. We wondered whether specific pathways, normally repressed by BCL6, became active under these conditions to maintain survival. Others have shown that genes normally repressed by BCL6 can contribute to survival specifically in ABC-DLBCL (7). To reveal pathways required for survival of BCL6-deficient DG75-AB7, which might prove to be important in ABC-DLBCL, we carried out a synthetic lethal screen of DG75-AB7 against a library of small molecule inhibitors, many of which are in clinical use or are candidates for clinical use, and sought a reduction in the surviving fraction of cells, which was greater than that produced by BCL6 deficiency alone.

Several agents from the library screen were found to enhance the effects of BCL6 deficiency. We chose to focus on lestaurtinib, a JAK2 inhibitor. JAK2 is activated in DLBCL (36) but has not previously been reported to be a direct target of BCL6 transcriptional repression. We produced several lines of evidence to support a direct effect of BCL6 on JAK2; 1) JAK2 mRNA levels increased in response to BCL6 deficiency, 2) BCL6 bound to the JAK2 promoter *in vivo* and *in vitro*, and 3) a BCL6 binding site in the JAK2 promoter region was required for BCL6-mediated repression in luciferase reporter assays.

We demonstrated that STAT3, a major target of phosphorylation by JAK2, was induced and phosphorylated in BCL6-deficient DG75-AB7. STAT3 mRNA expression is directly repressed by BCL67, and BCL6 also represses IL-6 production in macrophages to inhibit STAT3 signaling (45), but a role for BCL6 in regulating JAK2 has not been previously demonstrated. JAK-STAT signaling has been investigated in DLBCL; this pathway can be activated by IL-10 (36) and by diverse genetic mechanisms such as aberrant MYD88 signaling (6) or inactivating mutation of SOCS1 (46). Overall there may be constitutive STAT3 signaling in ~50% of DLBCL (3, 7), but activating mutations of JAK2 appear to be very rare, and mechanisms for JAK2 activation in DLBCL other than activating mutations have been suggested (47). Here we show that JAK2, like STAT3, is a direct BCL6 target gene in a Burkitt lymphoma cell line, and this raises the possibility that BCL6 contributes to the overall regulation of JAK2-STAT3 signaling.

It was surprising that JAK2 was not only increased in amounts on induction of BCL6 deficiency in DG75-AB7 but was also phosphorylated. We noted that IL10RA mRNA increased on induction of BCL6 deficiency in DG75-AB7, showing that it is directly or indirectly regulated by BCL6 (Table 1), and we wondered whether engagement of this receptor could mediate JAK2 phosphorylation. Experiments with IL10RA blocking antibodies supported the notion that BCL6 deficiency activated an IL10RA/JAK2/STAT3 pathway.

Our data suggested that an IL10RA/JAK2/STAT3 pathway is repressed by BCL6. IL10RA, JAK2, and STAT3 have been shown separately to be components of pathways that are specifically active in ABC-DLBCL. Both STAT3 (7) and IL10RA (29) have been suggested as targets for therapy in ABC-DLBCL, and ABC-DLBCL cell lines are more sensitive to JAK2 inhibition than GC-DLBCL cell lines (3). In addition, high serum IL10 levels carry a poor prognosis in DLBCL (36). Through our work we were able to link this disparate data to show that there is a role for BCL6 in the regulation of all these genes. Therefore, BCL6 appears to repress a survival pathway in ABC-DLBCL, and systematic future studies of BCL6 target genes might reveal other important survival mechanisms in ABC-DLBCL.

There has been interest in employing JAK2 inhibitors in DLBCL (48, 49), but the place of these agents has not been defined. We suggest that they might be useful adjuncts to conventional treatment in cases of ABC-DLBCL expressing relatively low levels of BCL6 and that BCL6 mRNA expression might be a component of a biomarker panel to predict patient populations that will benefit from these drugs.

Experimental Procedures

Construction of DG75-AB7—Both *BCL6* alleles of the parental EBV negative Burkitt lymphoma cell line, DG75-354 (gift of Dr. Berthold Henglein), which contains a tetracycline transactivator, were disrupted by homologous recombination, and a tetracycline repressible BCL6 cDNA was inserted to produce DG75-AB7. Exon 3, which contains the translation start site of *BCL6*, was disrupted (Fig. 1, *A* and *B*). The targeting construct contains a zeocin (zeo) resistance cassette that is flanked by *lox*P sites followed by a downstream SphI site with flanking arms of homology targeting it to the *BCL6* gene. The construct contains a unique KpnI restriction site facilitating linearization before gene targeting. After transformation of the parent DG75-354 cells *i.e.* DG75 containing a tetracycline transactivator construct, with this construct and subsequent selection in zeocin, targeted integration events were detected by PCR screening and confirmed by Southern blotting. Gene disruption was targeted to the 11763-bp genomic SphI fragment, which flanks exon 1b and finishes in exon 6. The arms of homology

were subcloned as a smaller fragment derived from this initial big construct. This 10-kb region was amplified from genomic DNA. This 9992-bp KpnI/SacII fragment was ligated into pBluescript KS+ (Stratagene), resulting in vector p10kb-homology. The 8918-bp ApaI/EagI fragment of p10kb-homology was then subcloned from p10kb-homology into pBluescript KS+ generating p8.9kb-homology. For disruption of the *BCL6* allele, a zeocin cassette was inserted into the SbfI site of p8.9kb-homology (end of exon 3). This 1245-bp zeocin cassette (including its promoter) was amplified from pCMV/*Zeo* utilizing primers adding *lox*P sites to both ends of the zeocin cassette and an SphI restriction site to its 3′ end. This SbfI-digested product was cloned into the SbfI site of p8.9kb-homology to generate the final targeting construct pTarg-*BCL6*. The orientation of the zeocin cassette was verified by restriction enzyme digestion, and the region surrounding the 5′ *lox*P site was sequenced. After targeting of the first *BCL6* allele, cells were transiently transfected with Cre-recombinase (pMC-Cre kindly supplied by H. Gu, University of Köln), which excised the region between the *lox*P sites. The premature stop codon generated by targeted *BCL6* gene disruption is likely to result in the mRNA being degraded by nonsense-mediated decay. The potential translation of the message would result in a 55-amino acid truncated protein, which was expected to be nonfunctional and quickly be degraded. Once the zeocin cassette and resistance was lost, the same targeting construct was used to knock-out the second allele.

Gene Expression Analysis—Gene expression changes due to the absence of BCL6 were measured by Affymetrix (Santa Clara, CA) microarrays. Total RNA was extracted using RNeasy minipreps (Qiagen, Hilden, Germany), and 100 ng of total RNA was processed with the GeneChip® Eukaryotic Whole Transcript Sense Target Labeling Assay kit (Affymetrix). Briefly double-stranded cDNA was synthesized from total RNA using random hexamers tagged with a T7 promoter sequence and transcribed *in vitro* by T7 RNA polymerase to produce antisense cRNA. This was subsequently purified and used as template for a further round of cDNA synthesis. After RNA hydrolysis, treatment of sense cDNA with uracil DNA glycosylase and apurinic/apyrimidinic endonuclease 1 (APE1) fragments the DNA strand. cDNA fragments are labeled by terminal deoxynucleotidyltransferase (TdT) with biotin and hybridized to the array (Human GeneChip 1.0 ST Array, Affymetrix), which was subsequently scanned.

The Quality of Microarray Data Were Evaluated by Box Plot and Scatter Plot Analysis—Real time RT-PCR-JAK2 and IL10RA mRNA levels were determined by real time PCR performed using an Applied Biosystems 7500 Real-Time PCR machine (Applied Biosystems, Foster City, CA) and Taqman Universal PCR Master Mix. JAK2 primers were: forward (5′-CAGGCAACAGGAACAAGATG) and reverse (5′-CCATTCCCATGCAGAGTCTT); IL10RA primers were forward (5′-CAGGAACTGACGGATTGGGAA) and reverse (5′-GCTTCAAACCACACAGACGG).

Small Molecule Inhibitor Screen—DG75-AB7 was seeded at a density of 5×10^4 cells/ml in a 384-well plate in a volume of 50 μl/well on day 0 and continuously cultured in the presence or absence of doxycycline (1 μg/ml) as well as a library of small molecule inhibitors (Table 4) for 4 days at which point cell survival was estimated. The small molecule library encompassed conventional chemotherapy and targeted therapy agents at four different concentrations. In total, six replica experiments were performed with the data from the replicas combined in the final analysis. Staurosporine (10 μM) was used as a positive control for the induction of apoptosis. Cell viability was estimated at the end of the experiment using the CellTiter-Glo (Promega, Southampton, UK) luminescence assay. 20 μl of CellTiter-Glo reagent was added to each well, the plate contents were mixed for 10 min at room temperature, and the luminescence was measured. Each culture condition was replicated six times. Raw luminescence values were $\log_2$-transformed and then z-score-standardized according to the $\log_2$ median effect and the variance of effects, which was estimated by calculation of the median absolute deviation.

Cell Culture, Growth, Cell Cycle, Flow Cytometry, and DNA Double-strand Break Analysis—Parental DG75 cells and its derivatives were cultured in RPMI media (Life Technologies) supplemented with 10% fetal calf serum (Lonza, Basel, Switzerland) and penicillin (10,000 units/ml) (Lonza) and streptomycin (10,000 μg/ml) (Lonza) and grown at 37 °C and 5% CO_2. Where indicated, doxycycline (1 μg/ml) (D9891; Sigma) in DMSO (D2650; Sigma) was added to the culture medium. For cell culture DG75-AB7 was cultured with doxycycline for 4 days, and inhibitors ruxolitinib and fedratinib (Selleck Chemicals, Houston, TX) and lestaurtinib (Tocris Bioscience, Bristol, UK) were added for 24 h.

Cells excluding trypan blue were counted, and cultures were split every 2 days so that concentrations did not exceed or fall below the preferred cell density of between 1 and 9×10^5 cells/ml. The doubling time (T_d) between time point 1 (t_1) and time point 2 (t_2) (in h) was calculated by inserting cell concentrations at time point t_1 (c_1) and time point t_2 (c_2) into the formula $T_d = (t_2 - t_1) \times (\ln_2/\ln(c_2/c_1))$.

For cell cycle analysis, 10^6 cells were collected by centrifugation, washed once in PBS, and resuspended in PBS (300 μl). Ice-cold ethanol (700 μl) was added, and the fixed cells were collected by centrifugation, washed once in PBS, and resuspended in 500 μl of PBS containing RNase A (0.2 mg/ml) (Qiagen) and digested at 37 °C for 1 h. Propidium iodide was added to a final concentration of 40 μg/ml, and cells were analyzed by flow cytometry.

Expression of IL10RA was determined by flow cytometry (FACSCanto, BD Biosciences) utilizing anti-IL10RA antibody (R&D Systems, Minneapolis, MN; MAB2742) in the presence of human Fc block (BD Biosciences; 564219). Detection was with secondary anti-mouse IgG-FITC (Jackson ImmunoResearch, West Grove, PA; 315-096-003). A blocking anti-IL10RA antibody (Novus Biologicals, Oxford, UK; NBP1–42534) was employed at 5 μg/ml to demonstrate functional effects. IL10 (R&D Systems) was employed at 10 ng/ml.

DG75-AB7 cells were cultured for 4 days in the presence or absence of doxycycline after which DNA double-strand breaks were induced by irradiation at a dose rate of 1 Gy/min at 250 kV constant potential and half-value layer of 1.5 mm copper (Pantak Industrial x-ray machine (Pantak Inc., East Haven, CT)). 2 h after irradiation DNA double-strand breaks were identified

using fluorescent detection of the phosphorylated form of H2AX (γH2AX). 5×10^5 cells were fixed using ice-cold ethanol for at least 24 h at 4 °C and then permeabilized with 0.1% Triton X-100 on ice for 10 min with 0.2 mg/ml RNase (Sigma; R6513); cells were then incubated at 37 °C for 1 h, blocked with 4% FCS, and stained with a 1:500 dilution of anti-γH2AX (Ser-139) (clone JBW301; Millipore 05–636) for 2 h on ice and then with a 1:200 dilution of secondary antibody (AlexaFluor488 goat anti-mouse IgG; Invitrogen A21121) with rotation at room temperature (in the dark) for 1 h. After washing, cells were stained with propidium iodide (0.5 μg/ml) and analyzed on a FACSCanto II (BD Biosciences) and characterized for cell cycle stage using FlowJo Software v7.6.4 (Treestar Inc., Ashland, OR). The mean fluorescent intensity of γH2AX was determined for cells within G_1 of the cell cycle.

Chromatin Immunoprecipitation—Binding of BCL6 to the JAK2 locus was analyzed by ChIP (carried out as described Papadopoulou *et al.* (30)) with an anti-BCL6 antibody (N3; Santa Cruz Biotechnology, Santa Cruz, CA), and the results were analyzed by real-time PCR. BCL6 binding to the CD20 locus was used as a control (31). JAK2 primers were forward (5′-ggttcattctcatccttcagat-3′) and reverse (5′-agtagaaagtgaggaggggtgt-3′).

Luciferase Reporter Assays—A 2.0-kb region upstream of the JAK2 transcription start site was cloned from DG75-AB7 genomic DNA. The gene was amplified by PCR using MyFi polymerase (Bioline, London, UK) and the primers 5′-taaggtaccccttgtccaccttg-3′ (forward, with a KpnI site) and 5′-cctgctagcttcgaactcagc-3′ (reverse, with a NheI site). The site was also cloned in the reverse orientation using the primers 5′-taagctagcccttgtccaccttg-3′ (forward, with a NheI site) and 5′-cctggtaccttcgaactcagc-3′ (reverse, with a KpnI site). The amplified product was digested with KpnI and NheI and cloned into the empty pGL4 Luciferase Reporter Vector, pGL4.10 (Promega, Fitchburg, WI). Site-directed mutagenesis was performed using the QuikChange II XL kit (Agilent, Santa Clara, CA) to create a mutated binding site, GGCCGAGAA. All mutations were confirmed by sequence verification. HEK-293 cells were transiently transfected with Turbofect transfection reagent (Thermo Scientific, Waltham, MA) following the manufacturer's instructions. Cells were seeded in 96-well white-bottomed plates 24 h before transfection. The cells were then co-transfected with BCL6-FLAG expression construct (50 or 100 ng) and/or empty pGL4.10 reporter vector to 200 ng total DNA. After 8 h the cells were then co-transfected with 100 ng of the various reporter constructs and 100 ng of pGL4.73 *Renilla* Luciferase construct. All transfections were performed in triplicate and luciferase activities were measured using the Dual-Glo Luciferase Assay System (Promega) 24 h after reporter construct transfection. All luminescence readings were normalized to *Renilla* luciferase control readings. Reporter assays (without co-transfection of BCL6 expression construct) were similarly carried out in DG75-AB7 in the presence and absence of doxycycline.

Western Blotting Analysis—DG75-AB7 cells were harvested and lysed in radioimmune precipitation assay buffer (150 mM sodium chloride, 1.0% Nonidet P-40, 0.5% sodium deoxycholate, 0.1% SDS, 50 mM Tris, pH 8.0) containing protease inhibitors (Sigma). Protein was separated by 7.5% SDS-PAGE (Bio-Rad). Gels were blotted to polyvinylidene difluoride membranes and probed with antibody. Anti-ATR (Abcam, Cambridge, UK; ab4471), anti-BLIMP1 (Cell Signaling Technology, Beverly, MA; #9115), anti-MYC (Cell Signaling Technology; #9402), anti-JAK2 (Cell Signaling Technology; #3230), anti-phospho-STAT3-Tyr-705 (Cell Signaling Technology; #9145), and anti-phospho-STAT3-Ser727 (Cell Signaling Technology; #9134) were all employed at 1:1000. Secondary anti-mouse IgG or anti-rabbit IgG were employed at 1:2000. Anti-STAT3 (Cell Signaling Technology; #9132) was employed at 1:2000, and secondary anti-rabbit IgG was employed at 1:5000.

Electromobility Shift Assays (EMSA)—EMSAs were carried out utilizing a LightShift Chemiluminescent EMSA kit (Thermo Scientific, Waltham, MA; 20148). EMSAs were performed using the LightShift Chemiluminescent EMSA kit (Thermo Scientific). Binding reactions containing 20 μg of nuclear protein lysate were preincubated for 15 min at room temperature in EMSA binding buffer (10 mM Tris, 50 mM KCl, 1 mM DTT, 10 mM $MgCl_2$, 10 μM $ZnCl_2$, 100 μg/ml BSA, 4% glycerol, 2 μg of Poly (dI·dC)) before the addition of a biotin-labeled probe and a subsequent 20-min incubation at room temperature. Complexes were separated on 5% Tris borate-EDTA polyacrylamide gels before electrophoretic transfer to nylon membranes and detection as per the manufacturer's instructions. For specific-competition analysis a 200-fold excess of unlabeled probe was added before the preincubation. For supershift analysis, 2 μg of antibody was incubated with the binding reaction for 20 min after the preincubation and before the addition of the labeled probe. The test probe was designed to the putative BCL6 binding site in the JAK2 promoter region (5′-ACGATTTCCTAGAATAAGTG-3′). The canonical BCL6 probe FB20 was used as a positive control (5′-GAAA-ATTCCTAGAAAGCATA-3′).

siRNA Knockdown—DG75-AB7 were transfected with siRNA directed against JAK2 (Life Technologies, 4392420) or a negative control siRNA (#4390843) using siPORT NeoFX (Life Technologies) after which they were cultured for 24 h. Doxycycline was then added to half the cells, which were then cultured for a further 24 h and harvested, and CellTiter-Glo luminescence (Promega) was determined.

In Vivo Adoptive Transfer—18–22-Week-old SCID-Beige mice (Charles River, Burlington, MA) were inoculated subcutaneously in the flank with DG75-AB7 (1×10^7 cells in 100 μl) premixed with equivolume amounts of Matrigel HC (Sigma, E1270) under general anesthesia. Tumors were left to establish for 7 days, and then the mice were assigned to one of four groups ($n = 8$). Group 1 received no treatment and regular drinking water and provided a baseline for tumor development and morphology. Group 2 received doxycycline (Sigma D9891) in the drinking water at 1 mg/ml. Group 3 received regular drinking water and once daily subcutaneous injections of lestaurtinib (10 mg/kg), and Group 4 received doxycycline in the drinking water (as before) in combination with once daily subcutaneous injections of lestaurtinib (10 mg/kg).

Lestaurtinib (LC Laboratories, Woburn, MA) was resuspended to a final concentration of 5 mg/ml in 40% PEG100 (Sigma 76293), 10% povidone C30 (Sigma P2472), and 2% ben-

zyl alcohol (Sigma 402834). Lestaurtinib was administered for 5 days of 7 (Monday to Friday) only. Due to some skin sensitivity the injection sites were rotated between the scruff and flanks.

All groups received water *ad libitum*, and the mean water intake per mouse was calculated (6.5 ml/mouse/day) corresponding to a mean dose of doxycycline ~300 mg/kg/mouse/day. No differences in fluid intake were noted between the groups. Animals were typically caged in single sex pairs, in conditions appropriate for immune-deficient mice (irradiated diet and bedding). After tumor initiation, body condition and tumor volumes were recorded daily, and water intake was monitored weekly. Tumor growth was monitored by measurement of the length (L) and the width (W) with Vernier calipers. Tumor volume was calculated by the formula volume $= W^2 \times 0.5$ liter.

When tumor volumes in two or more of the control mice exceeded 10 mm in size (in more than 2 dimensions), the experiment was terminated (under veterinary advice). Body mass and tumor mass measurements were made, and tissues were collected from all mice from all groups. All animal procedures were carried out in the Central Research Facility, University of Leicester, under the UK Home Office License Number PPL60/4399 and following National Cancer Research Institute guidelines with regard to maximum permissible tumor size.

Spleen samples were formalin-fixed (10% neutral-buffered formalin), dehydrated (70% ethanol), and impregnated with wax, and 4-μm sections were cut (following standard protocols). Staining with hematoxylin and the eosin was performed using Shandon Varistain staining machine according to the manufacturer's instructions.

The sections were dewaxed in xylene and rehydrated in alcohol. Antigen retrieval was carried out using a high temperature unmasking technique with diaminobenzidine chromagen solution (DAKO) high pH target retrieval solution in the microwave. Sections were quenched with peroxidase block, and sections were incubated with the monoclonal anti-BCL6 or anti-Ki-67 antibodies (DAKO) (1/10 dilution in TBS) for 45 min and rinsed with TBS/Tween buffer followed by incubation with the HRP-labeled polymer for 45 min and counterstaining with hematoxylin.

Author Contributions—R. B., D. B., S. E. E., J. Z., R. L. A., L. L., and R. E. carried out the experiments and analyzed the data. M. B. carried out the bioinformatics analysis. A. C. G. P., C. J. L., A. A., and S. D. W. analyzed the data and wrote the manuscript.

Acknowledgments—We are grateful to Dr. Berthold Henglein, CNRS UMR 7098, Université Pierre et Marie Curie, Paris, France for the gift of DG75-354 and to Drs. Katerina Hatzi and Ari Melnick for making ChIP-seq data available. Kate Lee (B/BASH, University of Leicester) provided bioinformatic support.

References

1. Lenz, G., Wright, G., Dave, S. S., Xiao, W., Powell, J., Zhao, H., Xu, W., Tan, B., Goldschmidt, N., Iqbal, J., Vose, J., Bast, M., Fu, K., Weisenburger, D. D., Greiner, T. C., *et al.* (2008) Stromal gene signatures in large-B-cell lymphomas. *N. Engl. J. Med.* **359,** 2313–2323
2. Iqbal, J., Greiner, T. C., Patel, K., Dave, B. J., Smith, L., Ji, J., Wright, G., Sanger, W. G., Pickering, D. L., Jain, S., Horsman, D. E., Shen, Y., Fu, K., Weisenburger, D. D., Hans, C. P., Campo, E., Gascoyne, R. D., *et al.* (2007) Distinctive patterns of BCL6 molecular alterations and their functional consequences in different subgroups of diffuse large B-cell lymphoma. *Leukemia* **21,** 2332–2343
3. Lam, L. T., Wright, G., Davis, R. E., Lenz, G., Farinha, P., Dang, L., Chan, J. W., Rosenwald, A., Gascoyne, R. D., and Staudt, L. M. (2008) Cooperative signaling through the signal transducer and activator of transcription 3 and nuclear factor-kB pathways in subtypes of diffuse large B-cell lymphoma. *Blood* **111,** 3701–3713
4. Lenz, G., Davis, R. E., Ngo, V. N., Lam, L., George, T. C., Wright, G. W., Dave, S. S., Zhao, H., Xu, W., Rosenwald, A., Ott, G., Müller-Hermelink, H.-K., Gascoyne, R. D., Connors, J. M., Rimsza, L. M., Campo, E., *et al.* (2008) Oncogenic CARD11 mutations in human diffuse large B cell lymphoma. *Science* **319,** 1676–1679
5. Davis, R. E., Ngo, V. N., Lenz, G., Tolar, P., Young, R. M., Romesser, P. B., Kohlhammer, H., Lamy, L., Zhao, H., Yang, Y., Xu, W., Shaffer, A. L., Wright, G., Xiao, W., Powell, J., Jiang, J.-K., *et al.* (2010) Chronic active B-cell-receptor signalling in diffuse large B-cell lymphoma. *Nature* **463,** 88–92
6. Ngo, V. N., Young, R. M., Schmitz, R., Jhavar, S., Xiao, W., Lim, K.-H., Kohlhammer, H., Xu, W., Yang, Y., Zhao, H., Shaffer, A. L., Romesser, P., Wright, G., Powell, J., Rosenwald, A., *et al.* (2011) Oncogenically active MYD88 mutations in human lymphoma. *Nature* **470,** 115–119
7. Ding, B. B., Yu, J. J., Yu, R. Y., Mendez, L. M., Shaknovich, R., Zhang, Y., Cattoretti, G., and Ye, B. H. (2008) Constitutively activated STAT3 promotes cell proliferation and survival in the activated B-cell subtype of diffuse large B-cell lymphomas. *Blood* **111,** 1515–1523
8. Li, Z., Wang, X., Yu, R. Y.-L., Ding, B. B., Yu, J. J., Dai, X.-M., Naganuma, A., Stanley, E. R., and Ye, B. H. (2005) BCL-6 negatively regulates expression of the NF-κB1 p105/p50 subunit. *J. Immunol.* **174,** 205–214
9. Chang, C. C., Ye, B. H., Chaganti, R. S., and Dalla-Favera, R. (1996) BCL-6, a POZ/zinc-finger protein, is a sequence-specific transcriptional repressor. *Proc. Natl. Acad. Sci. U.S.A.* **93,** 6947–6952
10. Ye, B. H., Cattoretti, G., Shen, Q., Zhang, J., Hawe, N., de Waard, R., Leung, C., Nouri-Shirazi, M., Orazi, A., Chaganti, R. S., Rothman, P., Stall, A. M., Pandolfi, P. P., and Dalla-Favera, R. (1997) The BCL-6 proto-oncogene controls germinal centre formation and Th2-type inflammation. *Nat. Genet.* **16,** 161–170
11. Dent, A. L., Shaffer, A. L., Yu, X., Allman, D., and Staudt, L. M. (1997) Control of inflammation, cytokine expression, and germinal center formation by BCL-6. *Science* **276,** 589–592
12. Offit, K., Lo Coco, F., Louie, D. C., Parsa, N. Z., Leung, D., Portlock, C., Ye, B. H., Lista, F., Filippa, D. A., and Rosenbaum, A. (1994) Rearrangement of the bcl-6 gene as a prognostic marker in diffuse large-cell lymphoma. *N. Engl. J. Med.* **331,** 74–80
13. Pasqualucci, L., Migliazza, A., Basso, K., Houldsworth, J., Chaganti, R. S., and Dalla-Favera, R. (2003) Mutations of the BCL6 proto-oncogene disrupt its negative autoregulation in diffuse large B-cell lymphoma. *Blood* **101,** 2914–2923
14. Wang, X., Li, Z., Naganuma, A., and Ye, B. H. (2002) Negative autoregulation of BCL-6 is bypassed by genetic alterations in diffuse large B cell lymphomas. *Proc. Natl. Acad. Sci. U.S.A.* **99,** 15018–15023
15. Duan, S., Cermak, L., Pagan, J. K., Rossi, M., Martinengo, C., di Celle, P. F., Chapuy, B., Shipp, M., Chiarle, R., and Pagano, M. (2012) FBXO11 targets BCL6 for degradation and is inactivated in diffuse large B-cell lymphomas. *Nature* **481,** 90–93
16. Pasqualucci, L., Dominguez-Sola, D., Chiarenza, A., Fabbri, G., Grunn, A., Trifonov, V., Kasper, L. H., Lerach, S., Tang, H., Ma, J., Rossi, D., Chadburn, A., Murty, V. V., Mullighan, C. G., Gaidano, G., Rabadan, R., Brindle, P. K., and Dalla-Favera, R. (2011) Inactivating mutations of acetyltransferase genes in B-cell lymphoma. *Nature* **471,** 189–195
17. Cerchietti, L. C., Hatzi, K., Caldas-Lopes, E., Yang, S. N., Figueroa, M. E., Morin, R. D., Hirst, M., Mendez, L., Shaknovich, R., Cole, P. A., Bhalla, K., Gascoyne, R. D., Marra, M., Chiosis, G., and Melnick, A. (2010) BCL6 repression of EP300 in human diffuse large B cell lymphoma cells provides a basis for rational combinatorial therapy. *J. Clin. Invest.* **120,** 4569–4582
18. Shaffer, A. L., Yu, X., He, Y., Boldrick, J., Chan, E. P., and Staudt, L. M. (2000) BCL-6 represses genes that function in lymphocyte differentiation, inflammation, and cell cycle control. *Immunity* **13,** 199–212

19. Tunyaplin, C., Shaffer, A. L., Angelin-Duclos, C. D., Yu, X., Staudt, L. M., and Calame, K. (2004) Direct repression of prdm1 by Bcl-6 inhibits plasmacytic differentiation. *J. Immunol.* **173,** 1158–1165
20. Reljic, R., Wagner, S. D., Peakman, L. J., and Fearon, D. T. (2000) Suppression of signal transducer and activator of transcription 3-dependent B lymphocyte terminal differentiation by BCL-6. *J. Exp. Med.* **192,** 1841–1848
21. Phan, R. T., Saito, M., Basso, K., Niu, H., and Dalla-Favera, R. (2005) BCL6 interacts with the transcription factor Miz-1 to suppress the cyclin-dependent kinase inhibitor p21 and cell cycle arrest in germinal center B cells. *Nat. Immunol.* **6,** 1054–1060
22. Shvarts, A., Brummelkamp, T. R., Scheeren, F., Koh, E., Daley, G. Q., Spits, H., and Bernards, R. (2002) A senescence rescue screen identifies BCL6 as an inhibitor of anti-proliferative p19(ARF)-p53 signaling. *Genes Dev.* **16,** 681–686
23. Ranuncolo, S. M., Polo, J. M., Dierov, J., Singer, M., Kuo, T., Greally, J., Green, R., Carroll, M., and Melnick, A. (2007) Bcl-6 mediates the germinal center B cell phenotype and lymphomagenesis through transcriptional repression of the DNA-damage sensor ATR. *Nat. Immunol.* **8,** 705–714
24. Phan, R. T., and Dalla-Favera, R. (2004) The BCL6 proto-oncogene suppresses p53 expression in germinal-centre B cells. *Nature* **432,** 635–639
25. Hammerschmidt, W., and Sugden, B. (1989) Genetic analysis of immortalizing functions of Epstein-Barr virus in human B lymphocytes. *Nature* **340,** 393–397
26. Maier, S., Santak, M., Mantik, A., Grabusic, K., Kremmer, E., Hammerschmidt, W., and Kempkes, B. (2005) A somatic knockout of CBF1 in a human B-cell line reveals that induction of CD21 and CCR7 by EBNA-2 is strictly CBF1 dependent and that down-regulation of immunoglobulin M is partially CBF1 independent. *J. Virol.* **79,** 8784–8792
27. Torrance, C. J., Agrawal, V., Vogelstein, B., and Kinzler, K. W. (2001) Use of isogenic human cancer cells for high-throughput screening and drug discovery. *Nat. Biotechnol.* **19,** 940–945
28. Kaelin, W. G. (2005) The concept of synthetic lethality in the context of anticancer therapy. *Nat. Rev. Cancer* **5,** 689–698
29. Béguelin, W., Sawh, S., Chambwe, N., Chan, F. C., Jiang, Y., Choo, J.-W., Scott, D. W., Chalmers, A., Geng, H., Tsikitas, L., Tam, W., Bhagat, G., Gascoyne, R. D., and Shaknovich, R. (2015) IL10 receptor is a novel therapeutic target in DLBCLs. *Leukemia* **29,** 1684–1694
30. Papadopoulou, V., Postigo, A., Sánchez-Tilló, E., Porter, A. C., and Wagner, S. D. (2010) ZEB1 and CtBP form a repressive complex at a distal promoter element of the BCL6 locus. *Biochem. J.* **427,** 541–550
31. Parekh, S., Polo, J. M., Shaknovich, R., Juszczynski, P., Lev, P., Ranuncolo, S. M., Yin, Y., Klein, U., Cattoretti, G., Dalla Favera, R., Shipp, M. A., and Melnick, A. (2007) BCL6 programs lymphoma cells for survival and differentiation through distinct biochemical mechanisms. *Blood* **110,** 2067–2074
32. Huang da, W., Sherman, B. T., and Lempicki, R. A. (2009) Bioinformatics enrichment tools: paths toward the comprehensive functional analysis of large gene lists. *Nucleic Acids Res.* **37,** 1–13
33. Huang, D. W., Sherman, B. T., Zheng, X., Yang, J., Imamichi, T., Stephens, R., and Lempicki, R. A. (2009) Extracting biological meaning from large gene lists with DAVID. *Curr. Protoc. Bioinformatics*, Chapter 13, Unit 13.11
34. Ci, W., Polo, J. M., Cerchietti, L., Shaknovich, R., Wang, L., Yang, S. N., Ye, K., Farinha, P., Horsman, D. E., Gascoyne, R. D., Elemento, O., and Melnick, A. (2009) The BCL6 transcriptional program features repression of multiple oncogenes in primary B-cells and is deregulated in DLBCL. *Blood* **113,** 5536–5548
35. Zhou, T., Georgeon, S., Moser, R., Moore, D. J., Caflisch, A., and Hantschel, O. (2014) Specificity and mechanism-of-action of the JAK2 tyrosine kinase inhibitors ruxolitinib and SAR302503 (TG101348). *Leukemia* **28,** 404–407
36. Gupta, M., Han, J. J., Stenson, M., Maurer, M., Wellik, L., Hu, G., Ziesmer, S., Dogan, A., and Witzig, T. E. (2012) Elevated serum IL-10 levels in diffuse large B-cell lymphoma: a mechanism of aberrant JAK2 activation. *Blood* **119,** 2844–2853
37. Hatzi, K., Jiang, Y., Huang, C., Garrett-Bakelman, F., Gearhart, M. D., Giannopoulou, E. G., Zumbo, P., Kirouac, K., Bhaskara, S., Polo, J. M., Kormaksson, M., MacKerell, A. D., Jr., Xue, F., Mason, C. E., Hiebert, S. W., *et al.* (2013) A hybrid mechanism of action for BCL6 in B cells defined by formation of functionally distinct complexes at enhancers and promoters. *Cell Rep.* **4,** 578–588
38. Lenz, G., Wright, G. W., Emre, N. C., Kohlhammer, H., Dave, S. S., Davis, R. E., Carty, S., Lam, L. T., Shaffer, A. L., Xiao, W., Powell, J., Rosenwald, A., Ott, G., Muller-Hermelink, H. K., Gascoyne, R. D., *et al.* (2008) Molecular subtypes of diffuse large B-cell lymphoma arise by distinct genetic pathways. *Proc. Natl. Acad. Sci. U.S.A.* **105,** 13520–13525
39. Niu, H., Ye, B. H., and Dalla-Favera, R. (1998) Antigen receptor signaling induces MAP kinase-mediated phosphorylation and degradation of the BCL-6 transcription factor. *Genes Dev.* **12,** 1953–1961
40. Niu, H., Cattoretti, G., and Dalla-Favera, R. (2003) BCL6 controls the expression of the B7–1/CD80 costimulatory receptor in germinal center B cells. *J. Exp. Med.* **198,** 211–221
41. Saito, M., Gao, J., Basso, K., Kitagawa, Y., Smith, P. M., Bhagat, G., Pernis, A., Pasqualucci, L., and Dalla-Favera, R. (2007) A signaling pathway mediating down-regulation of BCL6 in germinal center B cells is blocked by BCL6 gene alterations in B cell lymphoma. *Cancer Cell* **12,** 280–292
42. Cerchietti, L. C., Yang, S. N., Shaknovich, R., Hatzi, K., Polo, J. M., Chadburn, A., Dowdy, S. F., and Melnick, A. (2009) A peptomimetic inhibitor of BCL6 with potent anti-lymphoma effects *in vitro* and *in vivo*. *Blood* **113,** 3397–3405
43. Cerchietti, L. C., Ghetu, A. F., Zhu, X., Da Silva, G. F., Zhong, S., Matthews, M., Bunting, K. L., Polo, J. M., Farès, C., Arrowsmith, C. H., Yang, S. N., Garcia, M., Coop, A., Mackerell, A. D., Jr., Privé, G. G., and Melnick, A. (2010) A small-molecule inhibitor of BCL6 kills DLBCL cells *in vitro* and *in vivo*. *Cancer Cell* **17,** 400–411
44. Polo, J. M., Dell'Oso, T., Ranuncolo, S. M., Cerchietti, L., Beck, D., Da Silva, G. F., Prive, G. G., Licht, J. D., and Melnick, A. (2004) Specific peptide interference reveals BCL6 transcriptional and oncogenic mechanisms in B-cell lymphoma cells. *Nat. Med.* **10,** 1329–1335
45. Yu, R. Y.-L., Wang, X., Pixley, F. J., Yu, J. J., Dent, A. L., Broxmeyer, H. E., Stanley, E. R., and Ye, B. H. (2005) BCL-6 negatively regulates macrophage proliferation by suppressing autocrine IL-6 production. *Blood* **105,** 1777–1784
46. Mottok, A., Renné, C., Seifert, M., Oppermann, E., Bechstein, W., Hansmann, M. L., Küppers, R., and Bräuninger, A. (2009) Inactivating SOCS1 mutations are caused by aberrant somatic hypermutation and restricted to a subset of B-cell lymphoma entities. *Blood* **114,** 4503–4506
47. Witzig, T. E., Price-Troska, T. L., Stenson, M. J., and Gupta, M. (2013) Lack of JAK2 activating non-synonymous mutations in diffuse large B-cell tumors: JAK2 deregulation still unexplained. *Leuk. Lymphoma* **54,** 397–399
48. Younes, A., Romaguera, J., Fanale, M., McLaughlin, P., Hagemeister, F., Copeland, A., Neelapu, S., Kwak, L., Shah, J., de Castro Faria, S., Hart, S., Wood, J., Jayaraman, R., Ethirajulu, K., and Zhu, J. (2012) Phase I study of a novel oral janus kinase 2 inhibitor, SB1518, in patients with relapsed lymphoma: evidence of clinical and biologic activity in multiple lymphoma subtypes. *J. Clin. Oncol.* **30,** 4161–4167
49. Derenzini, E., and Younes, A. (2013) Targeting the JAK-STAT pathway in lymphoma: a focus on pacritinib. *Expert Opin. Investig. Drugs* **22,** 775–785
50. Rosenwald, A., Wright, G., Chan, W. C., Connors, J. M., Campo, E., Fisher, R. I., Gascoyne, R. D., Muller-Hermelink, H. K., Smeland, E. B., Giltnane, J. M., Hurt, E. M., Zhao, H., Averett, L., Yang, L., *et al.* (2002) The use of molecular profiling to predict survival after chemotherapy for diffuse large B-cell lymphoma. *N. Engl. J. Med.* **346,** 1937–1947